

Received: 2018.03.02
Accepted: 2018.04.28
Published: 2018.10.01

Altered DNA Methylation Sites in Peripheral Blood Leukocytes from Patients with Simple Steatosis and Nonalcoholic Steatohepatitis (NASH)

Authors' Contribution:
Study Design A
Data Collection B
Statistical Analysis C
Data Interpretation D
Manuscript Preparation E
Literature Search F
Funds Collection G

ABCDEF 1 **Jiayu Wu**
ABCD 1 **Ruinan Zhang**
AB 1 **Feng Shen**
AB 1 **Ruixu Yang**
AB 1 **Da Zhou**
AB 1 **Haixia Cao**
BCD 1 **Guangyu Chen**
ABD 1 **Qin Pan**
ADEG 1,2,3 **Jiangao Fan**

1 Department of Gastroenterology, Xinhua Hospital, Shanghai Jiao Tong University School of Medicine, Shanghai, P.R. China
2 Shanghai Key Laboratory of Children's Digestion and Nutrition, Shanghai, P.R. China
3 Shanghai Institute of Pediatrics, Shanghai, P.R. China

Corresponding Authors: Jiangao Fan, e-mail: fanjiangao@xinhuamed.com.cn, Qin Pan, e-mail: pan_qin@yeah.net

Source of support: This study was supported by the State Key Development Program for Basic Research of China (Ref: 2012CB517501), the National Natural Science Foundation of China (Refs: 81070322, 81270491, 81470840), and the 100 Talents Program of the Shanghai Board of Health (Ref: XBR2011007)

Background: The aim of this study was to identify DNA methylation sites in peripheral blood leukocytes from patients with histologically confirmed nonalcoholic fatty liver disease (NAFLD) that included simple hepatic steatosis and nonalcoholic steatohepatitis (NASH).





Material/Methods: DNA was isolated from peripheral blood leukocytes from patients with histologically diagnosed NAFLD (n=35), including simple hepatic steatosis (n=18) and NASH (n=17). Healthy controls included individuals without liver disease (n=30). DNA was hybridized, and DNA methylation was interrogated in an epigenome-wide association study (EWAS). DNA methylation levels (β -values) were correlated with serum lipid profiles, liver enzymes, and liver histology.

Results: Circulating blood leukocytes from 35 patients with NAFLD (simple steatosis and NASH) contained 65 CpG sites, which represented 60 genes that were differentially methylated when compared with healthy controls. In the simple hepatic steatosis group (n=18), 42 methylated CpG sites were found to be associated with increased levels of serum alanine aminotransferase (ALT), and 32 methylated CpG sites were associated with increased serum lipid profiles. In the NASH group (n=17), when compared with the simple hepatic steatosis group, methylated CpG sites showed significant correlations with the presence of lobular inflammation compared with hepatic steatosis and fibrosis. Six differentially methylated CpG sites were identified in the *ACSL4*, *CRLS1*, *CTP1A*, *SIGIRR*, *SSBP1* and *ZNF622* genes, which were associated with histologically confirmed simple hepatic steatosis and NASH.

Conclusions: The study identified some key methylated CpG sites from peripheral blood leukocytes, which might be used as serum biomarkers to stratify NAFLD patients into simple hepatic steatosis and NASH.

MeSH Keywords: **DNA Methylation • Epigenomics • Fatty Liver**

Full-text PDF: <https://www.medscimonit.com/abstract/index/idArt/909747>

 5627  8  5  40



Background

Nonalcoholic fatty liver disease (NAFLD) is defined as the pathological accumulation of fat in liver cells and tissues in the absence of hepatotoxicity due to alcohol intake or any other identified cause. NAFLD describes a spectrum of changes in the liver associated with fat accumulation that include simple hepatic steatosis, nonalcoholic steatohepatitis (NASH), fibrosis, and liver cirrhosis [1]. The global prevalence of NAFLD has been estimated to be as high as 25.2%, with the Middle East and South America showing the highest prevalence, and Africa has the lowest prevalence [2]. In Asia, the prevalence of NAFLD has been reported to have recently increased to 27.4% [3]. This high prevalence of NAFLD in Asia might be due to changes in lifestyle and dietary patterns, including the increasing availability of highly calorific convenience foods.

Simple hepatic steatosis is a mild form of NAFLD, which may progress to NASH in some cases. Progression to NASH has been reported in 44% of patients with simple hepatic steatosis at baseline [4]. In cases of NASH, up to 2.8% of patients may develop end-stage liver cirrhosis or hepatocellular carcinoma (HCC) [5]. Therefore, because the liver changes in NASH can be progressive and irreversible, NASH has become an increasingly common reason for liver transplantation [4]. Associations between NAFLD and insulin resistance, obesity, hyperlipidemia, type 2 diabetes, and metabolic syndrome have been shown [4]. However, the pathogenesis of NAFLD and the associated phenotypes remain to be elucidated.

The progression of NAFLD to cirrhosis and HCC is variable and modified by age, gender, genetic predisposition, and epigenetic factors. Despite being an invasive procedure associated with some degree of risk and dependency on adequate, relevant liver sampling, liver biopsy remains the gold standard for assessing all form of NAFLD. Optimal non-invasive detection methods for NAFLD are still being developed. However, a new approach for understanding the pathogenesis of NAFLD might be provided by identifying epigenetic modifications [6], which are known to be involved in insulin resistance (IR) and to affect lipid metabolism, and the liver cell endoplasmic reticulum and mitochondria due to oxidative stress responses [7].

DNA methylation occurs at the cytosine base within cytosine-guanine dinucleotides, which are referred to as CpG sites. During DNA methylation, DNA methyltransferase catalyzes the transfer of a methyl group to the fifth carbon atom from 5-methylcytosine within the cytosine ring, and an increased DNA methylation level of promoters that usually correlates with low or no transcription [8]. Also, the hypermethylation of the CpG islands is usually associated with gene silencing, and global hypomethylation of genomic DNA can affect genomic stability [9].

There have been few previously published studies on the potential role of DNA methylation in NAFLD. A study using a rodent model showed that diets depleted of methyl donors could promote DNA hypomethylation of important metabolism-related genes and that this hypomethylation altered hepatic fat metabolism, resulting in simple hepatic steatosis [10]. Recent research on human liver disease has begun to apply the genome-wide association studies (GWAS) [11,12], which have shown that alterations in the pattern of DNA methylation are capable of inducing gene expression changes that are reversible and can contribute to insulin resistance and changes in lipid metabolism [13]. The use of GWAS means that there is now the potential to detect epigenetic modifiers in NAFLD, which might provide molecular tools for diagnosing, assessing the severity, and predicting disease progression [14].

Recently, studies have explored the possibility of using circulating leukocytes, derived from peripheral blood samples, for the evaluation of potential biomarkers in liver disease [15]. A recent study by Nano et al., which was the most extensive study to date using circulating leukocytes, identified CpG sites and DNA methylation levels that were associated with serum enzyme levels and simple hepatic steatosis, resulting in new insights into the epigenetic mechanisms associated with NAFLD [16].

The aims of the present study were to identify DNA methylation sites in peripheral blood leukocytes in patients with histologically confirmed NAFLD, including simple hepatic steatosis and NASH. Of particular interest was the possibility that epigenetic changes in DNA methylation were associated with clinical parameters, including serum liver enzymes, and lipid profiles, as well as the histological features of NAFLD. The use of routine blood samples was combined with findings from liver biopsy histology, with the aim of determining whether circulating leukocytes could be used to identify specific methylated CpGs that could be related to liver enzyme levels, lipid profiles, or NAFLD phenotypes, to provide novel non-invasive biomarkers for NAFLD, but mainly for NASH in this study.

Material and Methods

Study participants and study design

Between March 2012 and May 2013, 35 Chinese Han patients with NAFLD between the ages of 18–70 years were recruited to the study in Shanghai, China. Also, 30 healthy controls with normal liver function tests were recruited. Individuals were excluded from the study if they reported excessive alcohol consumption (>30 g/day for men; >20 g/day for women) or had known diseases that could cause fatty liver, such as chronic hepatitis C, autoimmune hepatitis, drug-induced liver injury or Wilson's disease, who were being given total parenteral

nutrition (TPN), exhibited other end-stage diseases or malignancy, or who had diabetes mellitus. To ensure patient confidentiality, patient anonymity was included in the study protocol, and to meet the appropriate ethical requirements, all procedures were conducted in accordance with the ethical principles of the Declaration of Helsinki.

Evaluated clinical variables

All clinical variables were evaluated according to the normal reference standards of our institution. Venous blood samples and metabolic profiles were obtained from NAFLD patients and normal controls. The body mass index (BMI) was calculated using the weight (in kilograms) divided by the square of their height (in meters) (kg/m^2). The BMI classification used was the World Health Organization (WHO) classification for adults: lean individuals ($\text{BMI} < 18.5 \text{ kg}/\text{m}^2$), normal individuals ($\text{BMI} 18.5\text{--}24.9 \text{ kg}/\text{m}^2$), overweight individuals ($\text{BMI} 25.0\text{--}29.9 \text{ kg}/\text{m}^2$), and obese individuals ($\text{BMI} \geq 30 \text{ kg}/\text{m}^2$).

The following fasting blood biochemical tests were performed for all study participants using a conventional automated analyzer (Hitachi 7600, Tokyo, Japan): fasting blood glucose (FBG), insulin; total cholesterol (TC), triglyceride (TG), high-density lipoprotein cholesterol (HDL-C), low-density lipoprotein cholesterol (LDL-C), very low-density lipoprotein (VLDL). Liver function tests included alanine transaminase (ALT), aspartate transaminase (AST), γ -glutamyl-transpeptidase (GGT), total bilirubin (TBil), direct bilirubin (DBil), and uric acid (UA) levels.

The homeostatic model assessment insulin resistance (HOMA-IR) index was used to assess basal glucose and insulin concentrations. HOMA-IR scores were obtained by multiplying the fasting serum insulin level ($\mu\text{IU}/\text{mL}$) by the FBG level (mmol/L), and dividing the product by 22.5.

Each study participant underwent a FibroScan[®] 502 test (Echosens, Paris, France) with an M-probe to measure liver stiffness (kPa) and the controlled attenuation parameter (CAP) that correlated with liver fibrosis and steatosis, respectively. All 35 patients met the histological diagnostic criteria for NAFLD. All control subjects had a CAP value $< 240 \text{ dB}/\text{m}$ and a liver stiffness measurement (LSM) value $< 7.0 \text{ kPa}$, to confirm that they were free from fatty liver disease.

Liver histology

Patients with NAFLD ($n=35$) had undergone percutaneous liver biopsy with real-time ultrasound guidance. The liver biopsy specimens were fixed and stored in neutral buffered formalin, processed and embedded in paraffin wax blocks. The tissue sections were then cut onto glass slides. Hematoxylin and eosin (H&E) staining and Masson's trichrome staining for

collagen and reticulin were routinely performed on all biopsies, and the results were assessed under light microscopy by experienced histopathologists, who were unaware of the patient's clinical and imaging history. NAFLD, including simple liver steatosis and NASH, was diagnosed according to the semi-quantitative histological scoring algorithm of hepatic steatosis, hepatocyte ballooning, and lobular inflammation. A SAF score was created for each case including steatosis (S), activity (A, ballooning + lobular inflammation), and liver fibrosis (F). A score that fulfilled the criteria of $S \geq 1, A \geq 2, F_{\text{any}}$ was used to support the diagnosis of NASH [17].

DNA extraction and bisulfite conversion

DNA extraction from peripheral blood samples was performed using a nucleic acid extraction kit (Qiagen, Hilden, Germany). The quality of the DNA was determined using a NanoDrop 2000c spectrophotometer (Thermo Fisher Scientific Inc., DE, USA). Bisulfite conversion of the DNA (500 ng/sample) was then performed according to the manufacturer's protocol using the EZ DNA Methylation Kit (Zymo Research, CA, USA) and a modified thermo-cycling procedure (Illumina, San Diego, CA, USA).

DNA methylation status was analyzed with a microarray approach using the Illumina Human Methylation450 BeadChip platform (Illumina, San Diego, CA, USA) to interrogate DNA methylation in an epigenome-wide association study (EWAS). The methylation level of each cytosine was calculated as the fluorescence intensity ratio of the methylated alleles to the unmethylated alleles, based on the Infinium type I probes and the Infinium type II probes and was expressed as a β value. The β values ranged from between 0 (unmethylated) and 1 (completely methylated) according to the combination of the Cy3 and Cy5 fluorescence intensities [18]. Illumina Genome Studio[®] Methylation module version 1.0 (Illumina, San Diego, CA, USA) was used to calculate the β value for each CpG site. Color balance adjustment was performed to normalize the samples between the two color channels using Genome Studio Illumina software (V2010.3). GenomeStudio was used to normalize the data using different internal controls that were present on the Illumina HumanMethylation450 BeadChip platform (Illumina, San Diego, CA, USA).

All probes were subsequently filtered according to the following requirements: detection of P-values > 0.05 in one or more samples; the presence of single nucleotide polymorphisms (SNPs) at the 10 bp 3' end of the interrogating probe; and alignment with multiple locations on the X and Y chromosomes. The final number of valid CpG sites used for this study was 418,913. The global methylation level was compared between patients with NASH, patients with simple hepatic steatosis, and normal controls. The genomic distribution of the differentially methylated CpG sites was examined using the

distribution of the CpG sites among all analyzed sites on the Illumina HumanMethylation450 BeadChip platform.

Pyrosequencing

The methylation of specific cytosines with CpG dinucleotides was quantified by pyrosequencing using PyroMark Q 96 MD (Qiagen, Hilden, Germany). The acyl-CoA synthetase long-chain family member 4 (*ACSL4*) gene was used for validation. The sequencing primers were as follows: forward (GTGATGGATTTGGGGTTTT), reverse (AAAACCTCCCTAACCTCAATTAC). Sequencing primers (GTATTTAGAGGGTTAG AAGTTAT) were obtained using Pyromark Assay Design software (version 2.0) (Qiagen, Hilden, Germany). Bisulfite-treated DNA was amplified via polymerase chain reaction (PCR) using the PyroMark PCR Kit (Qiagen, Hilden, Germany) and PyroMark CpG software (Qiagen, Hilden, Germany) to present the sequencing results.

Kyoto Encyclopedia of Genes and Genomes (KEGG) pathway analysis

The Kyoto Encyclopedia of Genes and Genomes (KEGG) pathway database was used to analyze the effect of differentially methylated CpG sites and to identify signaling pathways that were significantly related to CpG sites (<http://www.genome.jp/kegg/pathway.html>). The method of detection of the false discovery rate (FDR) was used to exclude false-positive results [19,20].

Statistical analysis

Normally distributed data were expressed as the mean \pm standard deviation (SD) and as numbers and percentages. The non-normally distributed data were presented as the median and interquartile range (IQR). After methylation data pre-processing [21], the Illumina Methylation Analyzer (IMA) R software package was used to perform t-tests following methylation data pre-processing. The P-values were adjusted using the Benjamini-Hochberg false discovery rate (FDR) procedure for multiple comparisons, in which an FDR <5% was considered to be statistically significant. A multivariate linear regression model was used to analyze the associations between the DNA methylation levels of the identified genes and liver enzyme levels and lipid profiles as continuous variables, adjusted by gender, age and BMI. The potential associations between the histological features of NAFLD and DNA methylation levels were evaluated using Pearson's correlation coefficient (r). The diagnostic efficiencies of the candidate differentially methylated CpG sites were calculated through receiver-operating characteristic (ROC) curve analysis. An area under the curve (AUC) value >0.8 was interpreted as indicating very good efficiency, and an AUC value between 0.6–0.8 was interpreted as indicating good efficiency. All statistical analysis was

performed using SPSS software, version 17.0 (SPSS, IBM Inc., Chicago, IL). Statistical significance was based on P-values of <0.05. Statistically significant correlations were shown using plots generated with GraphPad Prism® software, version 6.0 C (GraphPad, La Jolla, CA, USA).

Results

Demographic, clinical, and metabolic characteristics of the study participants

The demographic, clinical, and metabolic characteristics of the participants in this study are presented in Table 1. Liver biopsies from 35 patients with NAFLD showed simple hepatic steatosis (n=18) and NASH (n=17), according to the SAF score. Among the total study participants (n=65), 30.8% were women (n=20). In addition to exhibiting changes in their serum laboratory profiles, patients with NAFLD presented increased serum levels of ALT, GGT, and UA, but showed no significant differences in FBG levels. In addition to presenting high serum levels of cytokokeratin (CK)18-M30 and CK18-M65, which are direct measures of liver cell damage, apoptosis, and inflammation, high LSM values were found, but only in patients with NASH.

The global pattern of methylated DNA CpG sites in NAFLD

Comparisons of global methylation levels in the peripheral blood leukocytes of patients with NAFLD phenotypes compared with the normal controls are shown in Figures 1 and 2. Among a total of 418,913 probes, the average DNA methylation levels were similar in the NASH, simple hepatic steatosis, and normal control groups in terms of their correlation with either the CpG site content or the gene nearest to their functional genome. Hypomethylation was observed in the region of CpG islands, its north shore and south shore area (Figure 1). Promoter areas were defined as transcription start site (TSS)1500, TSS200, the 5' UTR and the first exon. The DNA methylation levels were lower in promoter areas in all three groups studied (simple hepatic steatosis, NASH, and control groups) (Figure 2). The circulating blood leukocytes of the 35 patients with simple hepatic steatosis (n=18) and NASH (n=17) exhibited 65 CpG sites, which represented 60 genes that were differentially methylated, compared with normal controls. In the simple hepatic steatosis group, 42 methylated CpG sites were found to be associated with increased levels of alanine transaminase (ALT), and 32 methylated CpG sites were associated with increased serum lipid profiles, including TC, HDL-C, LDL-C, and TG levels. In the NASH group, compared with the simple hepatic steatosis group, methylated CpG sites showed more significant correlations with the presence of lobular inflammation than with hepatic steatosis and fibrosis.

Table 1. Clinical characteristics of the participants.

	NASH (n=17)	Simple hepatic steatosis (n=18)	NAFLD (n=35)	Control (n=30)	NAFLD vs. CL P-value
Sex (F) (N, %)	12 (70.6%)	15 (83.3%)	8 (22.9%)	12 (40.0%)	0.12**
BMI >25 (N, %)	12 (70.6%)	14 (77.8%)	26 (74.0%)	4 (13.0%)	<0.001**
Metabolic syndrome (N, %)	7 (41.2%)	6 (33.3%)	22 (63.0%)	0 (0.0%)	<0.001**
Central obesity (N, %)	13 (76.5%)	13 (72.2%)	26 (74.0%)	9 (30.0%)	0.01**
Age (y)	37.76±12.77	37.72±12.48	37.74±12.43	46.63±7.24	<0.001
HT (cm)	167.76±6.69	169.44±5.83	168.63±6.23	164.32±7.22	0.010
WT (kg)	76.88±11.15	79.97±13.38	78.47±12.27	62.29±9.04	<0.001
BMI	27.29±3.4	27.79±3.84	27.55±3.59	23.02±2.63	<0.001
FBG (mmol/L)	5.33±1.14	6.22±3.68	5.81±2.82	5.29±0.39	0.300
TBIL (μmol/L)	12.36±3.31	19.86±21.9	16.33±16.32	14.29±4.05	0.510
DBIL (μmol/L)	7.23±10.12	9.64±19.58	8.51±15.67	2.98±0.83	0.050
GGT (u/L)	78.25 (44.03–131.00)	51.55 (32.50–80.70)	65.35 (36.48–88.78)	13.00 (11.00–17.25)	0.020*
ALT (u/L)	70.48±40.78	75.61±64.31	73.19±53.79	15.6±4.42	<0.001
TC (mmol/L)	4.99±0.65	4.95±1.07	4.97±0.91	4.35±0.61	<0.001
TG (mmol/L)	2.37±2.13	2.01±0.77	2.17±1.5	0.82±0.34	<0.001
HDL-C (mmol/L)	1.23±0.34	1.19±0.28	1.21±0.3	1.43±0.25	<0.001
LDL-C (mmol/L)	2.8±0.66	3.08±0.82	2.97±0.76	2.24±0.38	<0.001
UA (μmol/L)	413.16±122.29	362.02±110.02	383.19±115.97	257.83±62.14	<0.001
CK18M 30 (ng/L)	537.44±317.21	362.03±162.21			<0.001***
CK18M 65 (ng/L)	1159.32±613.07	829.94±421.69			<0.001***
LSM (kpa)	9.45 (6.08–14.40)	5.70 (4.35–9.95)	7.60 (5.40–12.00)	4.15 (3.70–4.70)	<0.001*
CAP (dB/m)	328.50 (289.25–358.75)	310.00 (276.00–361.50)	310.00 (277.00–359.00)	195.00 (174.00–228.00)	<0.001*

* Mann-Whitney test; ** Pearson chi-square or Fisher's exact test; *** NASH vs. Simple Hepatic Steatosis P-value. FBG – fasting blood glucose; TC – total cholesterol; TG – triglyceride; HDL-C – high-density lipoprotein cholesterol; LDL-C – low-density lipoprotein cholesterol; ALT – alanine transaminase; AST – aspartate transaminase; GGT – γ -glutamyl-transpeptidase; TBIL – total bilirubin; DBIL – direct bilirubin; UA – uric acid; CK18 – cytokeratin-18; LSM – liver stiffness measurement; CAP – controlled attenuation parameter; N – number. Normal distribution data are expressed as the means±standard deviations and as numbers and percentages. The non-normal distribution data are presented as the median and interquartile range.

The 65 NAFLD-associated CpG sites, representing 60 genes, were found to be significantly methylated in individuals with NAFLD and normal controls based on a P-value of <0.05 and a false discovery rate (FDR) of $q < 0.05$ (Supplementary Table 1). The methylation levels (β values) in more than half of the CpG sites (41 sites, 65.1%) were within the range of 0–0.2, suggesting that hypomethylation mostly characterized the

NAFLD-associated CpG sites. Figure 3 shows the top 19 CpG sites associated with NAFLD presenting the most significant increases or decreases in methylation. Cg13291296 (coding *GPR125*) showed the most significant methylation level, with a 36% point change. Additionally, in an analysis of the difference in DNA methylation levels between patients with simple hepatic steatosis and normal controls, 119 CpG sites were

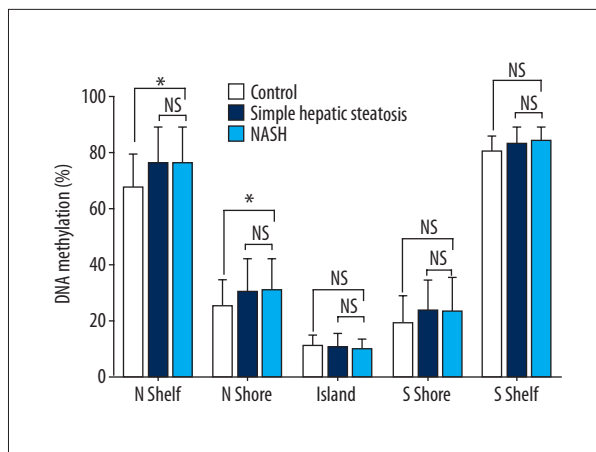


Figure 1. Global DNA methylation in circulating leukocytes from normal controls, patients with simple hepatic steatosis, and patients with nonalcoholic steatohepatitis (NASH), showing CpG island regions. Global DNA methylation is calculated as the average DNA methylation (%) at all CpG sites in each annotated region, according to the Illumina HumanMethylation450 BeadChip platform, which was used to interrogate DNA methylation in an epigenome-wide association study (EWAS). Shore, flanking regions of CpG islands (0–2,000 bp). Shelf, regions flanking island shores (2,000–4,000 bp from the CpG island). N – northern; S – Southern. * Significant difference ($P < 0.05$).

annotated to 106 genes (Supplementary Table 2). The gender of the study participant was not found to exert a statistically significant influence on methylation levels in this study.

Enrichment of gene-mapped CpG sites related to NAFLD in Kyoto Encyclopedia of Genes and Genomes (KEGG) pathways

Kyoto Encyclopedia of Genes and Genomes (KEGG) pathways were used to determine the enrichment of genes mapped to NAFLD-associated CpG sites before analyzing the association of clinical parameters with the NAFLD phenotypes (Supplementary Table 3). For the NAFLD-associated methylated CpG sites, the two top-ranked pathways involved ribosome biogenesis in eukaryotes ($EF=8.56$, $q=0.010$) and MAPK signaling ($EF=2.59$, $q=0.011$). Enriched genes related to metabolic pathways, cytokine-cytokine receptor interactions, and insulin signaling pathways were also found.

Because this study identified only 65 NAFLD-associated sites, all of these CpG sites were considered in the second KEGG pathway analysis for the association between DNA methylation and simple hepatic steatosis (Supplementary Table 4). This analysis identified genes that were mainly involved in vitamin digestion and absorption through enrichment factor (EF) analysis ($EF=15.84$, $q=0.033$) and in a particular pathway in cancer

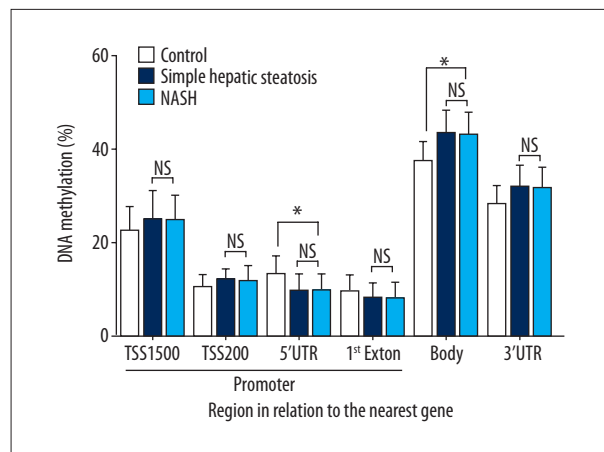


Figure 2. Global DNA methylation in circulating leukocytes from normal controls, patients with simple hepatic steatosis, and patients with nonalcoholic steatohepatitis (NASH) is shown for each gene region. Transcription start site (TSS) represents the proximal promoter, defined as 200 bp or 1,500 bp upstream of the TSS. * Significant difference ($P < 0.05$).

($EF=2.33$, $q=0.034$). After a search of the relevant literature, genes that were involved in the endoplasmic reticulum, insulin signaling, and adipose tissue homeostasis were identified. Although these associations showed a lower EF, they are recognized as being associated with the pathogenesis of NAFLD. These simple hepatic steatosis-associated methylated CpG sites, together with the NAFLD-associated methylated CpG sites mentioned above, were then used to explore the relationship between DNA methylation and clinical parameters.

Association between DNA methylation and liver enzyme and lipid profiles

The evaluation of the relationship between DNA methylation and clinical parameters focused on the NAFLD-associated CpG sites and the other 15 selected simple hepatic steatosis-associated CpG sites (in alphabetical order by gene name: *ABCC1*, *ATP5G1*, *AXIN2*, *CPT1A*, *CRLS1*, *DDX20*, *LDHB*, *MAPK1*, *NFE2L2*, *PMM1*, *PTEN*, *RB1*, *SEH1L*, *SGMS1*, and *SLCSA6*) from the KEGG pathway analysis. Simple linear regression analysis showed that most of the CpG sites were closely related to lipid profiles and ALT levels. Regarding demographic and clinical parameters, these CpG sites were strongly linked to BMI and waist circumference. Multivariate linear regression analysis adjusted for age, gender, and BMI also verified the results (significant results are listed in Supplementary Table 5).

A total of 42 methylated CpG sites were found to correlate with ALT levels, and these correlations remained significant after adjustment for age, gender, and BMI. Additionally, the correlations between levels of GGT with *cg03992938 (CCDC13)*,

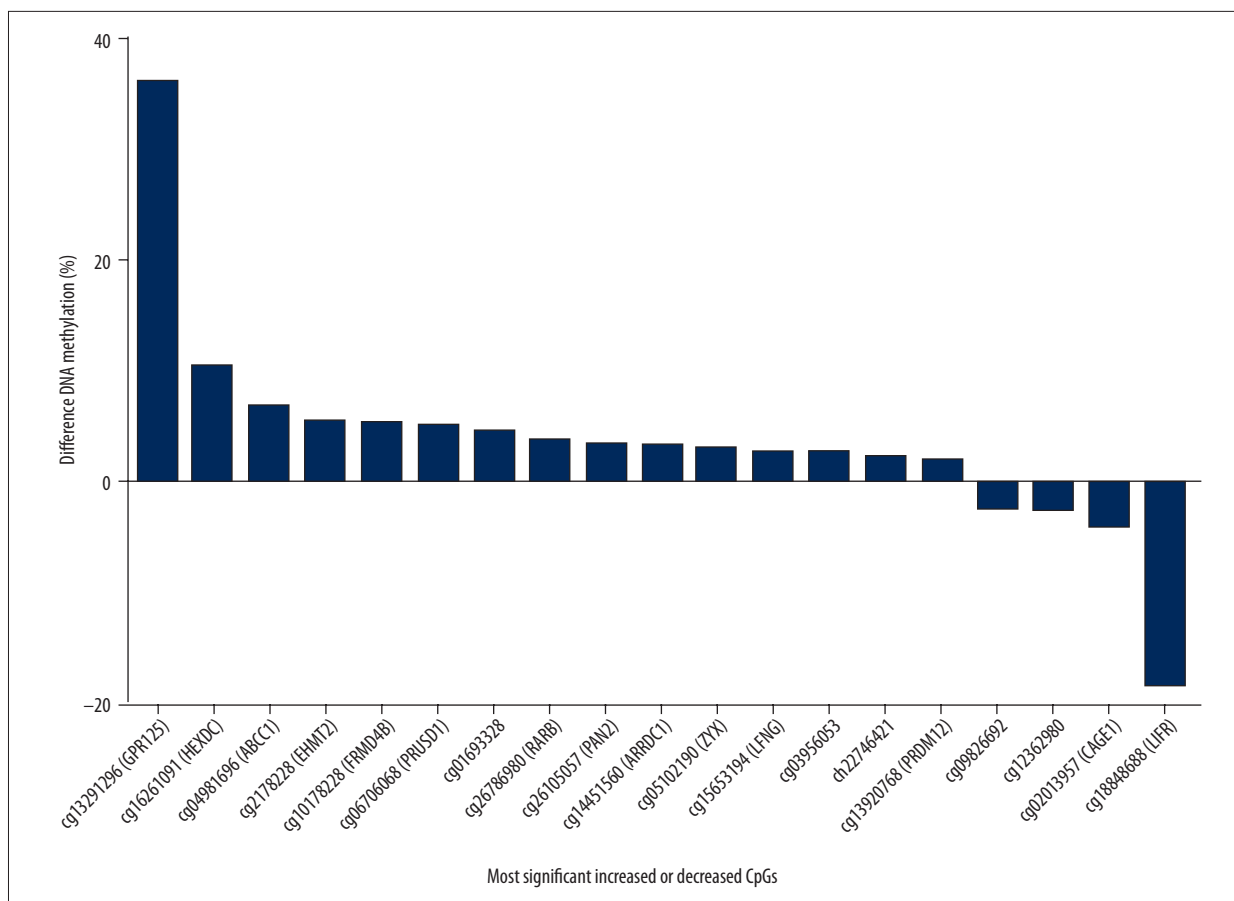


Figure 3. CpG sites showing the most significant increase or decrease in DNA methylation ($q < 0.05$) in nonalcoholic fatty liver disease (NAFLD).

cg04787602 (*C1orf183*), and cg014451560 (*ARRDC1*) were statistically significant. There were 32 CpG sites associated with TG, TC, or LDL-C levels, indicating dyslipidemia. With regard to glucose metabolism in NAFLD, the CpG sites were searched, and the results showed that cg07953400 (*PIGQ*), cg06706068 (*RPUSD1*), and cg16416718 (*CAMTA1*) exhibited strong correlations with fasting blood glucose levels, while cg25456633, cg03992938 (*CCDC13*), and cg02013957 (*CAGE1*) were closely associated with the homeostatic model assessment insulin resistance (HOMA-IR) index.

Methylation of CpG sites associated with NAFLD and liver histology

As shown in Table 2, a total of 23 CpG sites were partially correlated with the histological characteristics of NAFLD. Among the CpG sites associated with increased serum ALT levels, three sites were inversely correlated with hepatic steatosis: cg19634213 (*PTEN*) ($r = -0.358$, $P = 0.035$), cg01067963 (*MAPK1*) ($r = -0.343$, $P = 0.044$), and cg05102190 (*ZYX*) ($r = -0.357$, $P = 0.035$).

Additionally, seven CpG sites were negatively correlated with lobular inflammation: cg19634213 (*PTEN*) ($r = -0.37$, $P = 0.029$), cg16398128 (*ZNF622*) ($r = -0.497$, $P = 0.002$), cg22185268 (*COMMD4*) ($r = -0.341$, $P = 0.045$), cg22721468 (*SH3BP5L*) ($r = -0.337$, $P = 0.048$), cg15226170 (*PMM1*) ($r = -0.369$, $P = 0.029$), cg04787602 (*C1orf91*) ($r = -0.522$, $P = 0.032$), and cg05102190 (*ZYX*) ($r = -0.362$, $P = 0.033$). None of the ALT-associated CpG sites were found to be correlated with liver fibrosis.

Among the 32 CpG sites associated with lipid profiles, 11 were correlated with the histological characteristics of NAFLD: Cg00150500 (*HCFC1R1*) showed the strongest association with steatosis and lobular inflammation. Cg12473838 (*SSBP1*) showed a strong correlation with the following NAFLD histological features: steatosis ($r = -0.704$, $P < 0.001$), hepatocytes ballooning ($r = -0.542$, $P < 0.001$), lobular inflammation ($r = -0.531$, $P < 0.001$) and fibrosis ($r = -0.219$, $P < 0.001$). Additionally, cg13463639 (*SIGIRR*) and cg15653194 (*LFNG*) both showed a strong-to-moderate correlation with lobular inflammation ($r = 0.64$, $P < 0.001$ and $r = 0.485$, $P = 0.049$, respectively).

Table 2. Correlations(*r*) between methylation levels and histological parameters in NAFLD.

Illumina ID (n=35)	Steatosis		Ballooning		Inflammation		Fibrosis	
	<i>r</i>	<i>p</i>	<i>r</i>	<i>p</i>	<i>r</i>	<i>p</i>	<i>r</i>	<i>p</i>
cg15653194 (LFNG)	-0.179	0.491	-0.088	0.737	0.485	0.049*	-0.395	0.117
cg00150500 (HCFC1R1)	-0.381	0.024*	-0.337	0.048*	-0.346	0.042*	-0.179	0.303
cg04787602 (C1orf91)	0.286	0.265	0.382	0.131	-0.522	0.032*	0.355	0.161
cg16398128 (ZNF622)	-0.119	0.495	-0.031	0.859	-0.497	0.002*	-0.054	0.757
cg07112456 (LRWD1)	-0.526	0.025*	-0.439	0.069	-0.132	0.448	-0.095	0.708
cg01693328 (not mapped)	0.164	0.346	0.379	0.025*	0.288	0.093	0.21	0.226
cg15226170 (PMM1)	-0.222	0.199	0.032	0.854	-0.369	0.029*	-0.009	0.961
cg08013262 (INSR)	0.145	0.406	0.337	0.048*	0.047	0.788	0.083	0.635
cg10178228 (FRMD4B)	-0.085	0.629	0.048	0.785	-0.2	0.249	-0.062	0.723
cg05131957 (CRLS1)	-0.445	0.007*	-0.264	0.125	-0.448	0.007*	0.063	0.721
cg19634213 (PTEN)	-0.358	0.035*	-0.047	0.787	-0.370	0.029*	0.132	0.449
cg12473838 (SSBP1)	-0.704	0.001*	-0.542	0.001*	-0.531	0.001*	-0.219	0.001*
cg01067963 (MAPK1)	-0.343	0.044*	-0.165	0.344	-0.177	0.308	-0.002	0.992
cg22185268 (COMMD4)	-0.04	0.818	0.187	0.283	-0.341	0.045*	0.066	0.706
cg22721468 (SH3BP5L)	-0.19	0.275	-0.122	0.484	-0.337	0.048*	-0.078	0.654
cg13463639 (SIGIRR)	0.278	0.106	0.321	0.059	0.64	0.001*	0.230	0.184
cg13397649 (AFG3L2)	-0.375	0.138	-0.543	0.024*	0.093	0.722	-0.286	0.267
cg26309655 (TARS2)	0.294	0.252	0.558	0.020*	-0.399	0.113	0.2	0.441
cg04160753 (C10orf91)	-0.326	0.202	0.078	0.766	-0.486	0.048	-0.157	0.549
cg05102190 (ZYX)	-0.357	0.035*	-0.197	0.256	-0.362	0.033*	-0.064	0.716
cg00574958 (CTP1A)	0.134	0.441	0.294	0.087	0.443	0.008*	0.232	0.180
cg19878987 (LDHB)	-0.28	0.103	-0.048	0.784	-0.413	0.014*	0.116	0.507
cg15536552 (ACSL4)	0.482	0.050*	0.316	0.216	-0.385	0.127	0.339	0.183

* *p*<0.05.

No methylated CpG sites associated with FBG levels or HOMA-IR scores were correlated with the histological features of NAFLD. Pearson's correlation coefficient (*r*) (Y-axis) between the liver histology parameters (X-axis) and the methylated DNA sites that were inversely or directly associated with NAFLD are plotted in Figure 4.

Differentially methylated CpG (DMCpG) sites as potential biomarkers in NAFLD

The DNA methylation levels of the CpG sites that were correlated with the histological features of NAFLD were re-tested, which showed that the methylation levels of the *ACSL4*, *CRLS1*,

CTP1A, *SIGIRR*, *SSBP1*, and *ZNF622* genes were significantly different in patients with NASH compared with patients with simple hepatic steatosis. The areas under the receiver-operating characteristic (ROC) curves (AUROCs) for these six sites were 0.689 (95% CI, 0.556–0.821) for *ACSL4*, 0.742 (95% CI, 0.578–0.906) for *CRLS1*, 0.745 (95% CI, 0.581–0.910) for *CTP1A*, 0.882 (95% CI, 0.758–0.999) for *SIGIRR*, 0.817 (95% CI, 0.676–0.958) for *SSBP1*, and 0.735 (95% CI, 0.567–0.903) for *ZNF622* (Figure 5). These six sites showed significant effectiveness in discriminating between patients with NASH and patients with simple hepatic steatosis. The estimated cut-off values, sensitivities, specificities, positive predictive values (PPVs), and negative predictive values (NPVs) are listed in Table 3.

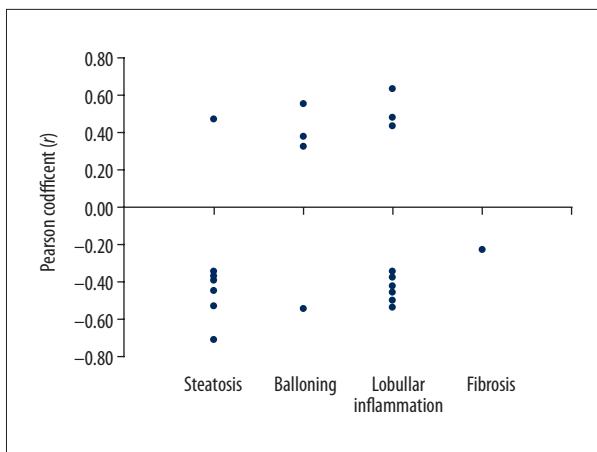


Figure 4. Pearson's correlation coefficients (r) (Y-axis) between histological features (X-axis) and methylated DNA sites inversely or directly associated with nonalcoholic fatty liver disease (NAFLD).

The effectiveness of these six sites was compared with that of serum CK18 M65 levels as a marker of inflammation and hepatocyte injury, and no significant differences were found.

Validation of *ACSL4* methylation by pyrosequencing

ACSL4 (cg15536552) was selected for validation through bisulfite pyrosequencing. The pyrosequencing results indicated that the methylation level of *ACSL4* (cg15536552) was consistent with that determined by the Illumina HumanMethylation450 BeadChip platform ($r=0.756$, $P<0.0001$). According to the SAF score, *ACSL4* was significantly hypomethylated in patients with NASH compared with patients with simple hepatic steatosis ($P=0.004$).

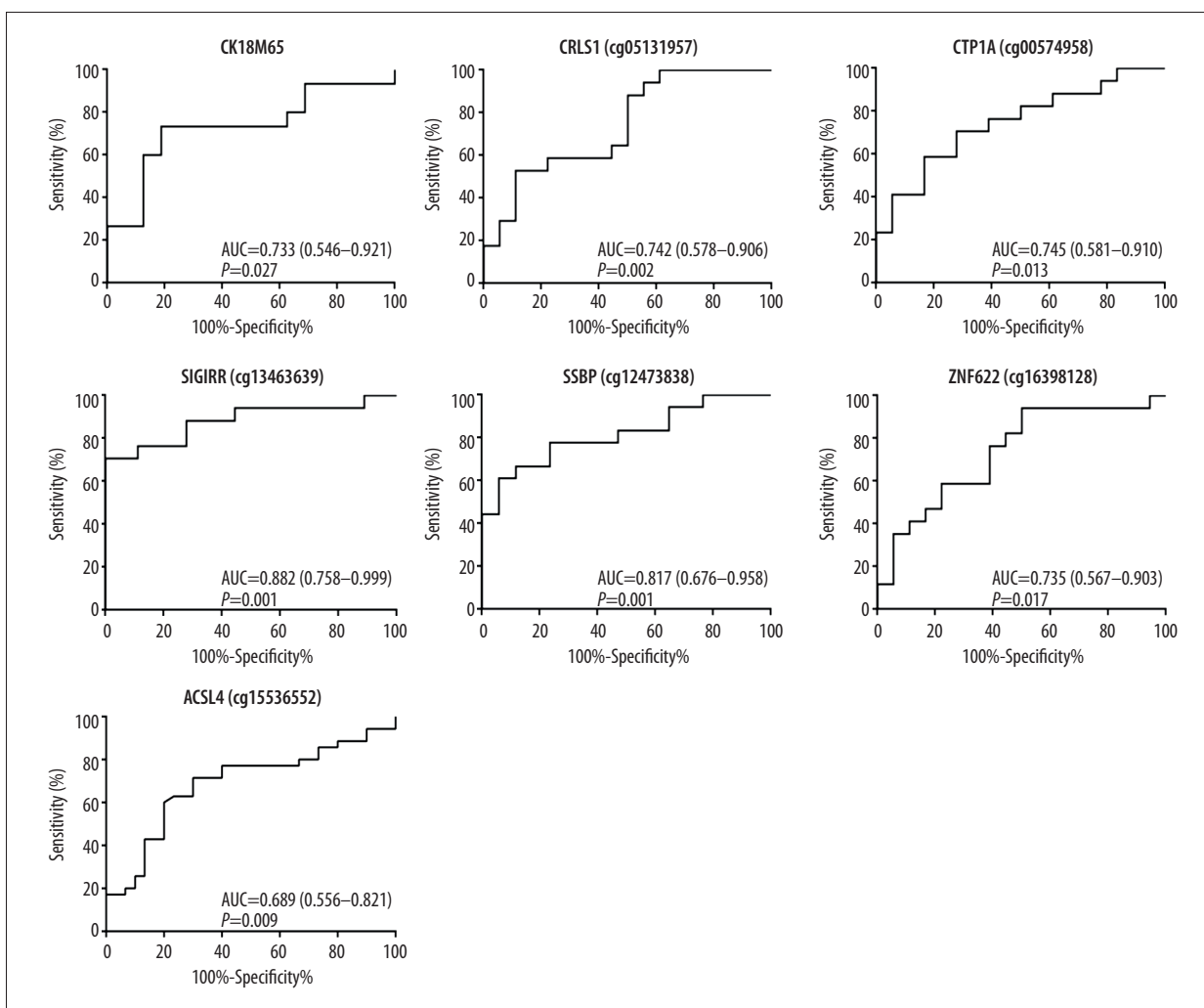


Figure 5. Receiver-operating characteristic (ROC) curves for the methylation levels of the nonalcoholic steatohepatitis (NASH)-related differentially methylated CpG sites.

Table 3. Comparison of the performance of each test for differentiating NASH versus simple hepatic steatosis.

Test	AUC (95%CI)	Sig	Cut-off	Sens (%)	Spec (%)	PPV (%)	NPV (%)	Z-score	P-value
CK18M65	0.733 (0.546–0.921)	0.027	756.35	73.3	75.0	78.6	76.5		
ACSL4	0.689 (0.556–0.821)	0.009	0.123	62.9	57.1	64.9	78.6	1.258	0.20
CTP1A	0.745 (0.581–0.909)	0.013	0.151	70.6	72.2	70.6	72.2	0.08	0.93
CRLS1	0.742 (0.578–0.906)	0.015	0.071	88.9	52.9	67.7	81.8	0.31	0.75
SIGIRR	0.882 (0.758–0.999)	0.001	0.787	70.6	99	92.3	77.3	1.12	0.26
SSBP1	0.817 (0.676–0.958)	0.001	0.04	61.1	94.1	91.7	69.6	0.32	0.75
ZNF622	0.735 (0.567–0.903)	0.017	0.046	50.0	94.1	92.3	61.5	0.08	0.93

AUROC – area under the receiver operating characteristic curve; Sens – sensitivity; Spec – specificity; PPV – positive predictive value; NPV – negative predictive value.

Discussion

Epigenetic processes are now recognized to play a role in the progression of nonalcoholic fatty liver disease (NAFLD). The characterization of how these epigenetic processes result in changes associated with liver injury provides new insights related to disease diagnostics and management. DNA methylation refers to the addition of a methyl group at a CpG site, which can influence the function of DNA by activating or suppressing gene expression [22]. CpG methylation is regarded as a ‘molecular clock’ during the progression of liver phenotypes from normal liver histology to simple hepatic steatosis to inflammation and fibrosis [23].

In the present study, the application of differentially methylated CpG sites to assess NAFLD phenotypes using microarrays allowed the analysis of a large fraction of the DNA methylome and the identification of genes correlated with changes in DNA methylation in peripheral blood leukocytes. This differential methylation may directly influence normal epigenetic regulation and cause pathological changes. The main purpose of the present study was to identify differentially methylated CpG sites in peripheral blood leukocytes to determine epigenetic biomarkers that might exhibit a strong correlation with the clinical parameters and histological features of NAFLD.

First, we analyzed more than 410,000 CpG sites to demonstrate that nonalcoholic steatohepatitis (NASH) was associated with differential DNA methylation in comparison with normal livers and simple hepatic steatosis. The adoption of a statistical significance of $q < 0.05$ enabled the identification of methylated sites that were significantly associated with NAFLD and simple hepatic steatosis. The identified NAFLD-associated CpG sites were mostly hypomethylated, a phenomenon supported by previous work by Murphy et al., who showed that the livers of individuals with advanced NAFLD exhibited more hypomethylation than those of individuals with mild NAFLD [13].

In this study, the top NAFLD-associated CpG sites, including *KCNQ3*, *FUT11*, *DUSP16*, *CAMTA1*, and *GTSE1*, appeared to present a close connection with NAFLD and a higher risk of developing HCC. Genes contributing to insulin resistance (*EHMT2*, *INSR*, *TARS2*, and *BRSK2*) and lipid metabolism (*RXRβ*) were enriched. Additionally, at simple hepatic steatosis-associated CpG sites, some adipogenic and lipid metabolism genes were also enriched in adipocytokine and insulin signaling pathways (*CPT1A*, *PTEN*, *LDHB*, *SGMS1*, *PMM1*, *ATP5G1*, *CRLS1*, and *PIGQ*). These observations provide evidence that, as a condition associated with metabolic disorders, NAFLD is influenced by integrated epigenetic modifications, even at an early stage. This finding might form the basis for future identification of DNA methylation biomarkers and their use to estimate future disease risk [24].

Increased serum levels of liver enzymes such as alanine aminotransferase (ALT), aspartate transaminase (AST), and γ -glutamyl-transpeptidase (GGT) are markers of liver injury [25]. GGT affects the pro-oxidant roles played by molecular species originating during the catabolism of glutathione and promotes lipid peroxidation. Previous studies have shown a genetic effect on liver enzyme levels [26]. In this study, the majority of the NAFLD-methylated CpG sites were associated with increased ALT levels, a connection that retained its significance even after adjustments for age, gender and body mass index (BMI). The analysis focused on the correlation of these CpG sites with the histological features of NAFLD. The differential methylation of CpG sites within *ZNF622*, *PTEN*, *COMMD4*, *SH3BP4L*, *PMM1*, *C1orf91*, and *ZYX* was associated with lobular inflammation. Some of these genes encode key enzymes that catalyze the initial steps of lipid, acetyl-CoA, and glucose metabolism and are members of insulin-like signaling pathways. Methylation differences in *ZYX* and *PTEN* were also correlated with steatosis, although no CpG sites associated with AST were identified.

The identification of methylation sites associated with liver enzymes and hepatic steatosis has recently been reviewed by Nano et al., who conducted an epigenome-wide association study and identified eight probes associated with serum GGT levels and one probe associated with serum ALT levels [16]. As in the present study, they identified no probe associated with serum AST levels.

Future large-scale studies may produce different results from the present study. Individuals with simple hepatic steatosis seldom progress to clinically significant liver disease and are considered to exhibit mild NAFLD. However, in patients with NASH, hepatic steatosis may trigger a fibrogenic repair process that can lead to cirrhosis or hepatocellular carcinoma (HCC). Murphy et al. found relevant differences in methylation that distinguished between patients with advanced fibrosis from those with mild fibrosis [13]. Although the present study employed the same technique for measuring DNA methylation, the approach taken for analyzing the differences between liver phenotypes was dissimilar. Also, our results supported the existence cross-talk between epigenetic features and liver enzymes at the identified CpG sites. Collectively, these observations may reflect the influential role of hepatic inflammation in simple hepatic steatosis at the epigenetic level, which contributes to progression toward NASH [27].

The second main aim of this study focused on the CpG sites correlated with lipid profiles. Dysfunctional lipid metabolism causes hepatic fat accumulation. Increased serum free fatty acids (FFA) cause increased triglyceride (TG) and very low-density lipoprotein (VLDL) levels in hepatocytes and trigger lipid peroxidation. These effects are closely related to the progression of NAFLD [28]. Also, circulating cytokine and adipokine levels as well as the associated mitochondrial dysfunction, lipotoxicity, endoplasmic reticulum damage and oxidative stress are involved in hepatic steatosis [29]. The most common pattern of dyslipidemia in NAFLD is characterized by hypertriglyceridemia, high levels of low-density lipoprotein cholesterol (LDL-C), and low levels of high-density lipoprotein cholesterol (HDL-C). In patients with NASH, there is a significant increase in the levels of oxidized LDL-C. In this study, a total of 31 CpG sites associated with LDL-C were selected after a multivariate analysis adjusted for gender, age, and BMI. Pearson's correlation coefficient (r) was used to verify the correlations between the CpG sites and NAFLD histological features. Ten of the identified CpG sites (*CTP1A*, *LFNG*, *ZNF622*, *HCFC1R1*, *CH3BP5L*, *COMMD4*, *SIGIRR*, *LDHB*, *SSBP1*, and *C10orf91*) were moderately correlated with lobular inflammation.

Previously published studies have shown that high serum levels of oxidized LDL can be considered a risk factor for NASH, as oxidized LDL-C interacts with immune cells and contributes to the inflammatory process, upregulates adhesion molecules,

and induces inflammation by increasing reactive oxygen species (ROS) generation and apoptotic cell death, which are involved in the progression of NASH [30]. In this study, DNA methylation was measured in peripheral blood leukocytes, and the results were consistent with the serum lipid profile data. According to Pearson's correlation coefficient (r) analysis, a close association was found between lobular inflammation and NAFLD-associated methylated CpG sites relevant to altered LDL-C levels, which might indicate that alterations in methylation levels also exert a direct or indirect influence on liver lobular inflammation that results in the onset of NASH.

The final part of this study highlighted six methylated CpG sites that differentiated NASH from simple hepatic steatosis (*ACLS4*, *CPT1A*, *CRLS1*, *SSBP1*, *SIGIRR*, and *ZNF622*). Cytokeratin (CK)18-M65 was selected as a reference standard, as it is one of the most commonly employed serum biomarkers for diagnosing NASH. A previously published meta-analysis showed that the area under the receiver-operating characteristic (AUROC) curve for CK18-M65 for the diagnosis of NASH was 0.71–0.93 (sensitivity 66%, specificity 82%) [31]. The present study showed that *SSBP1* and *SIGIRR* presented good efficiency for discriminating between NASH and simple hepatic steatosis, with AUCs of 0.817 and 0.882, respectively.

Expression of the *SSBP1* gene has been reported to be associated with the development of obesity and has been found to increase lipid accumulation in the liver. The cholesterol content of cells has been reported to be significantly increased following *SSBP1* knockdown, indicating that *SSBP1* could inhibit cellular cholesterol synthesis and accumulation [32]. *SIGIRR* (also known as *TIR8*) is a negative regulator of Toll-like receptor 4 (TLR4), which is upregulated in NAFLD and mediates NASH before the onset of liver fibrosis. The expression of the *SIGIRR* gene has also been shown to represent an important checkpoint in anti-cancer activity in natural killer (NK) cells [33].

Arachidonic acid preferred long-chain acyl-CoA synthetase (*ACSL4*) is a key enzyme involved in fatty acid metabolism in a variety of tissues and in hepatic steatosis, even after adjustment for BMI. Upregulation of the *ACSL4* gene accelerates lipogenesis, whereas downregulation of *ACSL4* prevents the accumulation of cellular cholesterol [34]. Previous study also reported leukocytic hypomethylated *ACSL4* an index for borderline/definitive NASH, with odds ratio (OR) at 11.44 and 95% confidence interval (CI) from 1.04 to 125.37 ($P=0.046$) [35]. In that study, the NAFLD Activity Score (NAS) scoring system has been used for the stratification of clinical phenotypes of NAFLD. However, inflammation facilitates fibrosis, while the prognosis of steatosis is still controversial. NAS scoring system is no longer recommended for the diagnosis of NASH because of its low prognostic value [36]. In our study, we used SAF score instead, a system that complements the histopathological

evaluation by dissociating hepatic steatosis from inflammation. This system helps to avoid some special cases from being excluded, as in some advanced cases, the liver may display ballooning and lobular inflammation with rare fat vacuoles, and provides a more accurate evaluation of NAFLD with better reproducibility [37]. In our study, *ACSL4* retains an effective diagnosis value with AUROC at 0.742 (0.578–0.906) for the stratification of NASH in NAFLD.

CPT1A is a protein-encoding gene that plays an important role in the mitochondrial transport of carnitine, which results in a decrease in fatty acid beta-oxidation, and DNA methylation of the CpG sites of the *CPT1A* gene has been reported to be associated with increased lipid levels and metabolic syndrome [38]. The *CRLS1* gene encodes cardiolipin, which is a phospholipid located in the inner mitochondrial membrane. The mitochondrial membrane is particularly susceptible to attack by ROS, resulting in damage to mitochondrial proteins, lipids and mitochondrial DNA, which can cause hepatocyte injury in NAFLD. Additionally, loss of cardiolipin leads to the generation of excessive levels of reactive oxygen species (ROS) that promote lipid peroxides and may cause oxidation of cardiolipin, catalyzed by cytochrome-c, resulting in apoptosis [39,40]. The *ZNF622* gene (also known as *ZPR9*) encodes a multiprotein that is involved in the apoptosis signal-regulating kinase 1 (ASK1) and transforming growth factor (TGF)- β signaling pathway, and down-regulation of ASK1 and TGF- β signaling activity can result in reduced intracellular lipid deposition.

Finally, this study identified a group of genes with a transcriptional status that was significantly correlated with DNA methylation levels, and this relationship differed between the NAFLD phenotypes. The findings of this study further showed that the methylated CpG sites detected in peripheral blood leukocytes were strongly associated with liver enzyme levels and lipid profiles, which are relevant to the outcomes of liver injury, impaired lipid metabolism, and the histological features of NAFLD. The findings of this study may have implications for the diagnosis of NAFLD, particularly for the diagnosis and evaluation of the severity of NASH, with differentially methylated CpG sites functioning as diagnostic or prognostic biomarkers. Epigenetic modifications might serve as malleable targets for future interventions that aim to detect or reverse advanced NAFLD.

The main challenge of this study was to assess the cause of NAFLD, as there was no evidence to explain why methylation facilitates lobular inflammation or why lobular inflammation in the progression of NASH alters methylation levels. All of these research questions require additional study. A further limitation of the study was that DNA methylation was measured in peripheral blood leukocytes, rather than in liver tissue, which may not be relevant to findings in the liver. Additionally, this study did not include gene expression analysis, and RNA samples were not available. As a result, differential DNA methylation was not studied directly from the analysis of the samples exhibiting the histological features of the NAFLD phenotypes. The whole-blood samples used in this study provided leukocytes for analysis, which were employed for quantifying DNA methylation levels, and allowed correlations with liver enzymes levels and lipid profiles to be assessed. Therefore, some CpG sites important to NAFLD might not have been detected in this study.

Conclusions

The findings of this clinical study showed that DNA methylation sites in peripheral blood leukocytes correlated with changes in serum liver enzyme levels and lipid profiles and with histologically confirmed forms of nonalcoholic fatty liver disease (NAFLD) that included simple steatosis and nonalcoholic steatohepatitis (NASH) when compared with healthy controls. The study identified six differentially methylated CpG sites in genes including *ACSL4*, *CPT1A*, *SSBP1*, *CRLS1*, *ZNF622*, and *SIGIRR* in NAFLD patients. In the simple hepatic steatosis group, 42 methylated CpG sites were found to be associated with the increased serum levels of alanine aminotransferase (ALT), and 32 methylated CpG sites were associated with the altered lipid profiles in the blood. In the NASH group, altered methylation of CpG sites showed a more close correlation with the presence of hepatic lobular inflammation, seen histologically on liver biopsy. These results suggest that changes in methylated CpG sites can be detected in peripheral blood leukocytes in patients with NAFLD, and these blood-based biomarkers may have potential value for clinical research and diagnosis of NASH.

Supplementary Tables

Supplementary Table 1. Individual CpG sites associated with NAFLD (q<0.05) in circulating leukocytes. (N=64).

Probe ID	p NAFLD	q NAFLD	NAFLD mean β	CL mean β	Difference (% points)	Gene symbol	UCSC RefGene Accession	Relation to gene region	Relation to CpG island
cg00150500	5.05E-08	0.003526	0.040611	0.026409	0.014201229	HCFC1R1; THOC6	NM_017885; NM_001002018; NM_001002017; NM_001142350; NM_024339	Body; TSS1500	Island
cg01693328	3.78E-06	0.037736	0.734933	0.689903	0.045030407				S_Shelf
cg02013957	2.80E-07	0.008217	0.069828	0.108342	-0.03851329	CAGE1; RIOK1	NM_205864; NM_031480; NM_001170693; NM_001170692	TSS1500; Body	S_Shore
cg03511638	7.43E-06	0.04944	0.207524	0.192478	0.015045277	FBXL15	NM_024326; NM_024326	1 st Exon; 5'UTR	Island
cg03615240	2.36E-06	0.029878	0.234903	0.217214	0.01768861				Island
cg03753066	2.57E-06	0.029878	0.042778	0.033719	0.009058818	PGPEP1	NM_017712	TSS200	N_Shore
cg03956053	4.68E-06	0.040684	0.094807	0.069568	0.025238064				Island
cg03992938	7.18E-06	0.04944	0.201834	0.1878	0.014034138	CCDC13	NM_144719; NM_144719	1 st Exon; 5'UTR	Island
cg04160753	5.99E-06	0.046488	0.275213	0.255442	0.019770564	C10orf91	NM_173541	TSS1500	
cg04396550	3.68E-12	1.54E-06	0.037964	0.025583	0.012380549	KCNQ3	NM_004519	TSS1500	Island
cg04787602	2.61E-07	0.008217	0.161306	0.144232	0.017073828	C1orf183	NM_198926; NM_019099	Body; TSS1500	Island
cg04981696	5.54E-07	0.012898	0.559923	0.491968	0.067954905	ABCC1	NM_019862; NM_019898; NM_019899; NM_004996; NM_019900	Body	S_Shore
cg05102190	7.38E-06	0.04944	0.292254	0.261536	0.030718122	ZYX	NM_003461; NM_001010972	TSS200	Island
cg06706068	6.62E-06	0.04866	0.450319	0.399254	0.051064413	RPUSD1	NM_058192	3'UTR	N_Shore
cg07067744	6.97E-06	0.04944	0.920563	0.90232	0.018243335	BRSK2	NM_003957	Body	
cg07112456	6.04E-07	0.013311	0.931972	0.912429	0.019543021	LRWD1	NM_152892	Body	S_Shelf
cg07953400	1.74E-06	0.02696	0.054226	0.045265	0.008961501	PIGQ	NM_004204; NM_148920	TSS1500; TSS1500	N_Shore
cg07956264	1.06E-07	0.006374	0.060192	0.042644	0.017547367	GPATCH3	NM_022078	1 st Exon	Island
cg08013262	2.14E-06	0.028915	0.051125	0.040134	0.010991397	INSR	NM_000208; NM_001079817	Body	Island
cg09367046	6.48E-06	0.048457	0.078046	0.057973	0.020073316	ANGEL1	NM_015305	TSS200	Island
cg09826692	3.66E-07	0.009581	0.695734	0.717446	-0.0217123				Island
cg10077144	6.43E-06	0.048457	0.151084	0.136608	0.014476221				Island
cg10178228	2.57E-06	0.029878	0.16383	0.11116	0.052670088	FRMD4B	NM_015123	TSS200	S_Shore
cg10576516	2.94E-07	0.008217	0.046487	0.034138	0.01234886	RECQL5; SAP30BP	NM_001003716; NM_013260; NM_001003715; NM_013260; NM_004259	TSS200; 1 st Exon; 5'UT	Island
cg12289509	9.38E-07	0.019426	0.12632	0.116298	0.010022888	TUBE1	NM_016262; NM_001033564	Body; TSS200	Island
cg12362980	3.73E-06	0.037736	0.890648	0.915371	-0.02472296				Island
cg13291296	1.94E-06	0.028151	0.928293	0.567811	0.360481701	GPR125	NM_145290	Body	
cg13373361	9.74E-07	0.019426	0.972063	0.958036	0.014027139	MYH16	NR_002147	Body	
cg13397649	2.39E-06	0.029878	0.184331	0.171045	0.013286234	AFG3L2	NM_006796	1 st Exon	Island

Probe ID	p NAFLD	q NAFLD	NAFLD mean β	CL mean β	Difference (% points)	Gene symbol	UCSC RefGene Accession	Relation to gene region	Relation to CpG island
cg13463639	1.14E-07	0.047685	0.795196	0.744952	0.050244062	SIGIRR	NM_001135053; NM_021805	TSS1500	S_Shore
cg13920768	4.76E-06	0.040684	0.180692	0.16038	0.02031251	PRDM12	NM_021619	3'UTR	Island
cg14214745	1.61E-06	0.025892	0.030079	0.02396	0.006119444	CRELD1	NM_001077415; NM_001031717; NM_015513; NM_015513; NM_001077415; NM_001031717	1 st Exon; 5'UTR	Island
cg14247318	2.91E-06	0.032137	0.06859	0.051255	0.017334521				S_Shore
cg14451560	4.08E-06	0.038185	0.163369	0.130014	0.033355016	ARRDC1	NM_152285	TSS1500	N_Shore
cg15317837	4.86E-06	0.0407	0.082077	0.065888	0.016188353	GTPBP4	NM_012341	TSS1500	Island
cg15653194	1.99E-09	0.000271	0.077077	0.051633	0.025443482	LFNG	NM_001166355; NM_002304; NM_001040168; NM_001040167	Body; TSS200	Island
cg16105594	1.46E-06	0.025002	0.222788	0.206881	0.015907317	MEF2C	NM_001131005; NM_002397	5'UTR; TSS1500	Island
cg16261091	5.26E-06	0.042403	0.871221	0.768176	0.103045403	C17orf101; HEXDC	NM_175902; NM_173620; NM_024648	Body; TSS1500	N_Shore
cg16357287	1.96E-07	0.007527	0.033464	0.022286	0.011177644	SEH1L	NM_001013437; NM_031216	TSS1500	N_Shore
cg16398128	1.66E-07	0.007527	0.038963	0.025503	0.01345955	ZNF622	NM_033414; NM_033414	5'UTR; 1 st Exon	Island
cg16416718	4.04E-06	0.038185	0.168379	0.155538	0.012840944	CAMTA1	NM_015215	TSS1500	Island
cg16487280	1.11E-06	0.020289	0.163618	0.146336	0.017282797	MYBL2	NM_002466	TSS1500	Island
cg17162475	1.08E-06	0.020289	0.136101	0.120308	0.015793168	C6orf150	NM_138441	TSS200	Island
cg17176517	5.44E-06	0.042966	0.055192	0.043187	0.012004537	SNX4	NM_003794; NM_003794	5'UTR; 1 st Exon	Island
cg18570553	3.67E-06	0.037736	0.144011	0.128948	0.015063351	PRR15	NM_175887	TSS200	N_Shore
cg18848688	1.42E-08	0.001192	0.143981	0.325489	-0.18150742	LIFR	NM_001127671; NM_002310	TSS1500; 5'UTR	Island
cg19137662	1.98E-07	0.007527	0.045624	0.032493	0.013131109	NOP56	NM_006392; NR_031699; NR_027700; NR_003078	Body; TSS200	Island
cg19189310	1.49E-06	0.025002	0.201487	0.18607	0.015416665	RPS10	NM_001014	5'UTR	Island
cg21786114	2.28E-07	0.007946	0.516219	0.460762	0.055456681	EHMT2	NM_006709; NM_025256	TSS1500	N_Shore
cg22185268	3.99E-07	0.009831	0.026994	0.020076	0.006918145	COMMD4	NM_017828	TSS200	Island
cg22402398	2.50E-06	0.029878	0.939115	0.923689	0.015425828	FGR	NM_001042747; NM_005248; NM_001042729	TSS1500; 5'UTR	
cg22598233	3.16E-06	0.033997	0.069128	0.056446	0.012681401	POLRMT	NM_005035	TSS200	Island
cg22721468	1.96E-06	0.028151	0.060214	0.04424	0.01597372	SH3BP5L	NM_030645	TSS1500	Island
cg22746421	1.52E-07	0.007527	0.87434	0.852661	0.021678989				
cg23224405	2.59E-09	0.000271	0.064945	0.045018	0.019927219	DUSP16	NM_030640; NM_030640	1 st Exon; 5'UTR	Island
cg24199050	2.65E-06	0.029971	0.010376	0.006359	0.004017477	GTSE1	NM_016426; NR_024009	TSS200	Island
cg24239690	7.36E-06	0.04944	0.196241	0.181611	0.014630372	FSCN1	NM_003088	Body	S_Shore
cg24689754	4.95E-06	0.0407	0.029538	0.020196	0.009341864	C19orf62	NM_001033549; NM_001033549; NM_014173; NM_014173	5'UTR; 1 st Exon	
cg25295726	1.84E-09	0.000271	0.181557	0.162827	0.018730389	FUT11	NM_173540	TSS200	Island
cg25456633	4.20E-06	0.038224	0.897003	0.878185	0.018817636				
cg25818813	4.10E-06	0.038185	0.064429	0.050092	0.014336947	MERTK	NM_006343	Body	Island

Probe ID	p NAFLD	q NAFLD	NAFLD mean β	CL mean β	Difference (% points)	Gene symbol	UCSC RefGene Accession	Relation to gene region	Relation to CpG island
cg26105057	2.02E-06	0.028151	0.160883	0.126787	0.034095982	PAN2	NM_014871; NM_001166279; NM_001127460; NM_014871; NM_001166279	1 st Exon; 5'UTR; TSS200	Island
cg26309655	4.66E-06	0.040684	0.16828	0.148223	0.02005632	TARS2	NM_025150	TSS200	
cg12473838	4.88E-06	0.028795	0.040501	0.031202	0.009299747	SSBP1	NM_003143; NR_015392	TSS200; Body	Island
cg26786980	6.79E-06	0.049042	0.220594	0.183155	0.037438788	RARB	NM_016152; NM_016152; NM_000965; NM_000965	5'UTR; 1 st Exon	

Supplementary Table 2. Individual CpG sites associated with simple hepatic steatosis (q<0.05) in circulating leukocytes. (N=119).

Probe ID	p Simple hepatic steatosis	q Simple hepatic steatosis	Simple hepatic steatosis mean β	CL mean β	Difference (% points)	Gene symbol	UCSC RefGene accession	Relation to gene region	Relation to CpG island
cg00150500	0.00000	0.00005	0.04354	0.02641	0.01713	HCFC1R1; THOC6	NM_017885; NM_001002018; NM_001002017; NM_001142350; NM_024339	Body; TSS1500	Island
cg00574958	0.00000	0.02625	0.13777	0.19441	-0.05664	CPT1A; CPT1A	NM_001876; NM_001031847	5'UTR	N_Shore
cg00639286	0.00001	0.03794	0.11783	0.09329	0.02454	ATOX1	NM_004045	Body	Island
cg00932007	0.00000	0.02625	0.07328	0.04803	0.02525	SERINC1; PKIB	NM_020755; NM_181794; NM_020755	1 st Exon; TSS200; 5'UTR	Island
cg01067963	0.00001	0.02968	0.06460	0.04919	0.01541	MAPK1	NM_138957; NM_002745	TSS1500	Island
cg01216607	0.00001	0.04888	0.13731	0.11167	0.02564	ZNHIT1; PLOD3	NM_006349; NM_001084; NM_001084	TSS1500; 1 st Exon; 5'UTR	Island
cg01525244	0.00000	0.00830	0.22203	0.17144	0.05059	CBX7	NM_175709	TSS200	N_Shore
cg01801101	0.00000	0.02176	0.31191	0.27460	0.03730	AMZ1	NM_133463	5'UTR	N_Shore
cg02432888	0.00001	0.03410	0.92622	0.93604	-0.00982	SMARCA4	NM_001128845; NM_001128844; NM_001128848; NM_001128848; NM_001128846; NM_003072; NM_001128849; NM_001128847	1 st Exon; Body	N_Shelf
cg02581963	0.00000	0.00977	0.09723	0.06908	0.02816	C10orf75	NR_026762	TSS200	Island
cg03027241	0.00000	0.01712	0.35425	0.42982	-0.07557	KCNG1	NM_002237	3'UTR	Island
cg03069383	0.00001	0.04806	0.22846	0.20088	0.02758	RDH14	NM_020905	1 st Exon	Island
cg03074984	0.00001	0.04262	0.22030	0.19083	0.02947	RPS6KA4	NM_003942; NM_001006944	TSS200	Island
cg03511638	0.00000	0.02698	0.21013	0.19248	0.01765	FBXL15	NM_024326; NM_024326	1 st Exon; 5'UTR	Island
cg03956053	0.00000	0.00468	0.10087	0.06957	0.03130				Island
cg03992938	0.00000	0.02085	0.20399	0.18780	0.01619	CCDC13	NM_144719; NM_144719	1 st Exon; 5'UTR	Island
cg04396550	0.00000	0.00000	0.03999	0.02558	0.01440	KCNQ3	NM_004519	TSS1500	Island
cg04551440	0.00000	0.02375	0.06975	0.05204	0.01771	KATNAL1	NM_001014380; NM_032116	TSS200; 5'UTR	Island

Probe ID	p Simple hepatic steatosis	q Simple hepatic steatosis	Simple hepatic steatosis mean β	CL mean β	Difference (% points)	Gene symbol	UCSC RefGene accession	Relation to gene region	Relation to CpG island
cg04672769	0.00000	0.01712	0.10358	0.08340	0.02017	HARS	NM_002109; NM_012208; NM_002109	5'UTR; TSS200; 1stExon	Island
cg04699668	0.00000	0.02654	0.78765	0.83452	-0.04687				N_Shore
cg04781764	0.00000	0.01704	0.86144	0.88530	-0.02387	WDR51B	NM_172240	Body	
cg04787602	0.00000	0.02085	0.16300	0.14423	0.01876	C1orf183; C1orf183	NM_198926; NM_019099	Body; TSS1500	Island
cg04851352	0.00001	0.04156	0.32402	0.30766	0.01637				Island
cg04981696	0.00000	0.01712	0.55926	0.49197	0.06730	ABCC1	NM_019862; NM_019898; NM_019899; NM_004996; NM_019900	Body	S_Shore
cg05020775	0.00001	0.03145	0.11804	0.09411	0.02393	SNPH	NM_014723	TSS200	Island
cg05102190	0.00000	0.01712	0.30075	0.26154	0.03922	ZYX	NM_003461; NM_001010972	TSS200	Island
cg05131957	0.00000	0.02625	0.08817	0.06755	0.02062	CRLS1; CRLS1	NM_019095; NM_019095; NM_001127458	1st Exon; 5'UTR; TSS1500	Island
cg05209527	0.00001	0.03018	0.20213	0.15172	0.05042	SLC5A6	NR_028323; NM_080592; NM_021095; NM_016085; NM_001170795	TSS1500; Body; 5'UTR	S_Shore
cg05377161	0.00001	0.04888	0.11639	0.09404	0.02235				Island
cg05629721	0.00000	0.02654	0.29331	0.24457	0.04875	PSMB8	NM_004159; NM_148919; NM_004159	5'UTR; TSS1500; 1st Exon	S_Shore
cg05977109	0.00000	0.02085	0.09199	0.06838	0.02361	SGMS1	NM_147156	5'UTR	Island
cg06276429	0.00001	0.04156	0.21157	0.17132	0.04025	SLC39A7; RXRB	NM_006979; NM_021976; NM_001077516	TSS1500; Body	N_Shore
cg07067659	0.00001	0.03187	0.03402	0.02441	0.00961	SLC7A5	NM_003486	1st Exon	Island
cg07112456	0.00001	0.03536	0.93287	0.91243	0.02044	LRWD1	NM_152892	Body	S_Shelf
cg07953400	0.00001	0.02968	0.05508	0.04526	0.00982	PIGQ	NM_004204; NM_148920	TSS1500	N_Shore
cg07956264	0.00000	0.00228	0.06267	0.04264	0.02003	GPATCH3	NM_022078	1st Exon	Island
cg08180934	0.00000	0.02625	0.05768	0.04568	0.01200	STRAP	NM_007178	TSS200	Island
cg08276889	0.00000	0.02375	0.03778	0.02814	0.00964	LOC100133985	NR_024444	Body	Island
cg08730728	0.00001	0.04156	0.10524	0.07919	0.02606				Island
cg09090048	0.00001	0.03018	0.21230	0.18139	0.03091	VPS26B; NCAPD3	NM_052875; NM_015261	TSS1500; Body	Island
cg09267087	0.00001	0.04156	0.67624	0.64183	0.03441				
cg09367046	0.00001	0.04262	0.07982	0.05797	0.02184	ANGEL1	NM_015305	TSS200	Island
cg09457469	0.00000	0.01698	0.06248	0.04671	0.01577	YBX2	NM_015982	Body	Island
cg09826692	0.00000	0.02375	0.69472	0.71745	-0.02273				Island
cg10059171	0.00001	0.03187	0.07502	0.05829	0.01674	GPR89B	NM_016334; NM_016334	5'UTR; 1st Exon	Island
cg10178228	0.00000	0.00820	0.17082	0.11116	0.05966	FRMD4B	NM_015123	TSS200	S_Shore
cg10369688	0.00001	0.03018	0.15684	0.13906	0.01778	ZFP36	NM_003407	Body	Island
cg10381071	0.00000	0.01712	0.15437	0.20650	-0.05213	TLE3	NM_020908; NM_001105192; NM_005078	TSS1500	Island

Probe ID	p Simple hepatic steatosis	q Simple hepatic steatosis	Simple hepatic steatosis mean β	CL mean β	Difference (% points)	Gene symbol	UCSC RefGene accession	Relation to gene region	Relation to CpG island
cg10576516	0.00000	0.00019	0.05003	0.03414	0.01589	RECQL5; SAP30BP	NM_001003716; NM_013260; NM_001003715; NM_013260; NM_004259	TSS200; 1 st Exon; 5'UTR	Island
cg10965669	0.00001	0.02931	0.80870	0.82408	-0.01538	AXIN2	NM_004655	Body	Island
cg11319362	0.00001	0.04251	0.08666	0.06828	0.01838	ARL6IP5	NM_006407; NM_006407	1 st Exon; 5'UTR	Island
cg11542063	0.00000	0.02625	0.05513	0.03884	0.01629	NFE2L2	NM_006164; NM_006164; NM_001145413; NM_001145412	5'UTR; 1 st Exon; TSS1500	Island
cg11866422	0.00000	0.02654	0.06337	0.05160	0.01177				Island
cg12289509	0.00001	0.04442	0.12657	0.11630	0.01027	TUBE1; C6orf225	NM_016262; NM_001033564	Body; TSS200	Island
cg12362980	0.00000	0.00307	0.88730	0.91537	-0.02807				Island
cg12407666	0.00000	0.02901	0.12378	0.10250	0.02128	RIC8B	NM_018157	TSS1500	Island
cg12810189	0.00001	0.03920	0.04387	0.03696	0.00691	BCAP29	NR_027830; NM_018844; NM_018844; NM_001008405	Body; 1 st Exon; 5'UTR; TSS1500	Island
cg12850793	0.00000	0.02321	0.15979	0.14310	0.01669	DENND5A	NM_015213	TSS200	Island
cg13110034	0.00001	0.03187	0.07293	0.06148	0.01145	ANKRD34A; POLR3GL	NM_001039888; NM_032305	TSS1500; 5'UTR	Island
cg13199615	0.00001	0.03018	0.23755	0.21115	0.02640	KRTCAP2; TRIM46	NM_173852; NM_025058	TSS1500; Body	N_Shore
cg13398864	0.00000	0.02433	0.11061	0.08598	0.02463	SEC22A	NM_012430	TSS200	N_Shore
cg13485756	0.00000	0.02698	0.09370	0.08224	0.01146	RB1	NM_000321	TSS200	Island
cg14022530	0.00000	0.02698	0.07371	0.05385	0.01986	SASS6; CCDC76	NM_194292; NM_019083	TSS200	Island
cg14214745	0.00000	0.01698	0.03114	0.02396	0.00718	CRELD1	NM_001077415; NM_001031717; NM_015513; NM_015513; NM_001077415; NM_001031717	1 st Exon; 5'UTR	Island
cg14247318	0.00001	0.03018	0.06991	0.05126	0.01865				S_Shore
cg15043926	0.00000	0.02698	0.28089	0.26430	0.01659	STIM2	NM_001169117; NM_020860; NM_001169118	Body	Island
cg15226170	0.00000	0.02879	0.37491	0.31659	0.05832	PMM1	NM_002676	TSS1500	S_Shore
cg15324256	0.00000	0.02625	0.05617	0.04062	0.01555	QTRTD1; KIAA1407	NM_024638; NM_020817	TSS1500; 1 st Exon	Island
cg15324448	0.00000	0.02625	0.10020	0.08001	0.02019	ZNF643	NM_023070	TSS200	Island
cg15536552	0.07584	0.04796	0.20583	0.34740	-0.01416	ACSL4	NM_022977; NM_004458	5'UTR; 5'UTR	N_Shore
cg15572086	0.00000	0.01698	0.06120	0.04806	0.01314	C1orf203	NR_027645; NR_024126; NR_024124; NR_027646; NR_024125	TSS1500	Island
cg15653194	0.00000	0.00394	0.07660	0.05163	0.02496	LFNG	NM_001166355; NM_002304; NM_001040168; NM_001040167	Body; TSS200	Island
cg16007711	0.00000	0.01712	0.11104	0.08414	0.02689	RHOBTB2	NM_001160036; NM_001160037; NM_015178	Body; 5'UTR	S_Shore
cg16306148	0.00001	0.03359	0.01234	0.00608	0.00626	YBX1	NM_004559	TSS1500	Island

Probe ID	p Simple hepatic steatosis	q Simple hepatic steatosis	Simple hepatic steatosis mean β	CL mean β	Difference (% points)	Gene symbol	UCSC RefGene accession	Relation to gene region	Relation to CpG island
cg16357287	0.00000	0.00228	0.03588	0.02229	0.01360	SEH1L; SEH1L	NM_001013437; NM_031216	TSS1500	N_Shore
cg16398128	0.00000	0.00000	0.04360	0.02550	0.01810	ZNF622	NM_033414; NM_033414	5'UTR; 1 st Exon	Island
cg16416718	0.00000	0.02879	0.16998	0.15554	0.01445	CAMTA1	NM_015215	TSS1500	Island
cg16743070	0.00000	0.01721	0.04222	0.02640	0.01582	MYST3	NM_001099413; NM_001099412; NM_006766	5'UTR	Island
cg16803522	0.00000	0.01441	0.03705	0.02603	0.01102	RASGRP1	NM_001128602; NM_005739	TSS1500	Island
cg17074213	0.00001	0.02901	0.20986	0.15861	0.05125	TGFBR3	NM_003243; NM_003243	1 st Exon; 5'UTR	Island
cg17162475	0.00000	0.02375	0.13817	0.12031	0.01786	C6orf150	NM_138441	TSS200	Island
cg17168242	0.00000	0.01599	0.09273	0.08238	0.01035	OTUD7B	NM_020205	TSS200	Island
cg17176517	0.00001	0.04039	0.05653	0.04319	0.01334	SNX4	NM_003794; NM_003794	5'UTR; 1 st Exon	Island
cg17427781	0.00001	0.04227	0.08943	0.07059	0.01884	DDX20; C1orf183	NM_007204; NM_198926	TSS200; Body	Island
cg18676790	0.00001	0.03018	0.27930	0.34935	-0.07005				
cg18848688	0.00001	0.02968	0.14296	0.32549	-0.18253	LIFR	NM_001127671; NM_002310	TSS1500; 5'UTR	Island
cg19050851	0.00000	0.02690	0.03973	0.02876	0.01097	ARSB	NM_000046; NM_198709	Body; Body	Island
cg19137662	0.00000	0.01441	0.04705	0.03249	0.01455	NOP56	NM_006392; NR_031699; NR_027700; NR_003078	Body; TSS200; TSS1500	Island
cg19362196	0.00000	0.02625	0.70650	0.76251	-0.05601	STMN1	NM_005563; NM_203399; NM_203401; NM_001145454	TSS1500	Island
cg19520115	0.00000	0.00160	0.12095	0.10488	0.01607	CAPZB	NM_004930	Body	Island
cg19634213	0.00000	0.01712	0.05716	0.04074	0.01643	PTEN; KILLIN	NM_000314; NM_001126049	TSS1500; 1 st Exon	Island
cg19693031	0.00001	0.03187	0.80756	0.85146	-0.04390	TXNIP	NM_006472	3'UTR	
cg19878987	0.00000	0.02280	0.10362	0.08020	0.02342	LDHB	NM_002300	TSS1500	S_Shore
cg20656751	0.00000	0.02625	0.51357	0.47261	0.04096	NAT8L	NM_178557	1stExon	Island
cg21012729	0.00001	0.03763	0.08208	0.06527	0.01681	NIN	NM_182946; NM_020921; NM_182944	5'UTR	Island
cg21373806	0.00001	0.04156	0.83546	0.86386	-0.02840	BAHCC1	NM_001080519	Body	N_Shore
cg21786114	0.00001	0.03187	0.51357	0.46076	0.05281	EHMT2	NM_006709; NM_025256	TSS1500	N_Shore
cg22185268	0.00000	0.00217	0.02871	0.02008	0.00864	COMMD4	NM_017828	TSS200	Island
cg22721468	0.00000	0.00228	0.06494	0.04424	0.02070	SH3BP5L	NM_030645	TSS1500	Island
cg22746421	0.00000	0.01712	0.87645	0.85266	0.02379				
cg22902478	0.00001	0.04156	0.10027	0.08525	0.01502	LOC100130987	NR_024469	TSS200	Island
cg23224405	0.00000	0.00011	0.06783	0.04502	0.02281	DUSP16	NM_030640; NM_030640	1 st Exon; 5'UTR	Island
cg23348158	0.00000	0.01712	0.09342	0.06174	0.03168	FUZ	NM_025129	TSS200	S_Shore
cg23512165	0.00000	0.02085	0.02886	0.02041	0.00845	MTMR4	NM_004687; NM_004687	1 st Exon; 5'UTR	Island
cg24108286	0.00001	0.03145	0.25285	0.21178	0.04107	TFDP1	NR_026580; NM_007111	TSS1500	

Probe ID	p Simple hepatic steatosis	q Simple hepatic steatosis	Simple hepatic steatosis mean β	CL mean β	Difference (% points)	Gene symbol	UCSC RefGene accession	Relation to gene region	Relation to CpG island
cg24689754	0.00000	0.02433	0.03045	0.02020	0.01026	C19orf62	NM_001033549; NM_001033549; NM_014173; NM_014173	5'UTR; 1 st Exon	
cg24728479	0.00001	0.03187	0.19258	0.17546	0.01712	ZNF252; C8orf77	NR_023392; NR_026974	TSS1500; Body	Island
cg25053907	0.00001	0.02968	0.06377	0.05198	0.01179	ZNF721; PIGG	NM_133474; NM_017733; NM_001127178; NM_133474	5'UTR; TSS200; 1 st Exon	Island
cg25295726	0.00000	0.01101	0.18162	0.16283	0.01879	FUT11	NM_173540	TSS200	Island
cg25678532	0.00000	0.02625	0.05138	0.03889	0.01249	RBBP8	NM_203291; NM_203292; NM_002894	TSS1500; TSS200	Island
cg25818813	0.00000	0.02014	0.06671	0.05009	0.01661	MERTK	NM_006343	Body	Island
cg25856120	0.00001	0.04680	0.11157	0.08244	0.02914	ATP5G1	NM_005175; NM_005175; NM_001002027	1 st Exon; 5'UTR	S_Shore
cg25989057	0.00001	0.02942	0.03813	0.02660	0.01154	AIP	NM_003977	TSS200	Island
cg26309655	0.00001	0.04156	0.17136	0.14822	0.02314	TARS2	NM_025150	TSS200	
cg26462136	0.00001	0.03647	0.08411	0.06628	0.01783	ATXN7L3	NM_001098833; NM_020218	TSS1500	Island
cg26791384	0.00001	0.04156	0.25191	0.21622	0.03569	SYCE1L	NM_001129979	Body	Island
cg26824705	0.00001	0.04888	0.08142	0.06402	0.01740	MUL1	NM_024544	TSS200	Island
cg27164612	0.00000	0.02654	0.01342	0.00813	0.00529				
cg27612695	0.00000	0.02625	0.18852	0.15615	0.03238	SUZ12P	NR_024187	Body	S_Shore

Supplementary Table 3. Significantly enriched KEGG pathways of genes with altered DNA methylation level in NAFLD.

Pathway ID	Description	p Value	q Value	Genes	Enrich factor
hsa03008	Ribosome biogenesis in eukaryotes	0.004	0.010	GTPBP4	GTP binding protein4
				NOP56	Ribonucleo protein
hsa04010	MAPK signaling pathway	0.001	0.011	DUSP16	Dual specificity phosphatase 16
				MEF2C	Myocyte enhancer factor 2C

Supplementary Table 4. Significantly enriched KEGG pathways of genes with altered DNA methylation level in simple hepatic steatosis.

Pathway ID	Description	p Value	q Value	Genes	Enrich factor
hsa04977	Vitamin digestion and absorption	0.0007	0.033	SLC5A6	Solute carrier family 5 member 6
				ABCC1	ATP binding cassette sub familyC member1
hsa03013	RNAtransport	0.0100	0.040	DDX20	DEAD-box helicase 20
				SEH1L	SEH1 like nucleoporin
hsa05200	Pathways in cancer	0.0070	0.034	PTEN	Phosphatase and tensin homolog
				AXIN2	Axin 2
				MAPK1	Mitogen-activated protein kinase 1
				RB1	RB transcriptional corepressor 1

Supplementary Table 5. Significance of associations between biological parameters and selected methylated CpG sites.

Illumina ID	Gene symbol	GLU		HOMAIN		TG		TC		HDL		LDL		GGT		ALT		AST	
		1#	2#	1#	2#	1#	2#	1#	2#	1#	2#	1#	2#	1#	2#	1#	2#	1#	2#
cg00150500	HCFC1R1	0.492	0.736	0.290	0.433	0.020	0.545	0.008	0.027*	0.505	0.516	0.000	0.005*	0.107	0.132	0.006	0.057	0.792	0.668
cg00574958	CTP1A	0.333	0.435	0.433	0.768	0.001	0.001*	0.017	0.308	0.067	0.575	0.000	0.001*	0.125	0.417	0.034	0.478	0.340	0.657
cg01067963	MAPK1	0.321	0.685	0.520	0.963	0.039	0.795	0.216	0.632	0.070	0.316	0.018	0.259	0.365	0.201	0.006	0.035*	0.603	0.454
cg01693328		0.899	0.875	0.408	0.665	0.247	0.816	0.126	0.170	0.173	0.441	0.087	0.165	0.162	0.174	0.002	0.009*	0.111	0.185
cg01801101	AMZ1	0.971	0.949	0.392	0.838	0.006	0.211	0.240	0.280	0.287	0.844	0.016	0.078	0.983	0.932	0.000	0.002*	0.818	0.488
cg02013957	CAGE1	0.860	0.788	0.010	0.010*	0.049	0.371	0.213	0.951	0.051	0.656	0.150	0.413	0.133	0.122	0.001	0.024*	0.498	0.082
cg03511638	FBXL15	0.158	0.282	0.136	0.258	0.129	0.930	0.585	0.985	0.373	0.908	0.073	0.446	0.113	0.141	0.010	0.070	0.588	0.818
cg03615240		0.147	0.757	0.286	0.355	0.101	0.206	0.036	0.142	0.816	0.237	0.012	0.012*	0.179	0.400	0.000	0.033*	0.061	0.373
cg03992938	CCDC13	0.107	0.296	0.067	0.032*	0.844	0.139	0.035	0.449	0.404	0.240	0.001	0.006*	0.016	0.021*	0.012	0.011*	0.187	0.882
cg04160753	C10orf91	0.162	0.316	0.936	0.880	0.014	0.105	0.030	0.161	0.466	0.798	0.014	0.108	0.295	0.361	0.104	0.345	0.904	0.986
cg04787602	C1orf183	0.153	0.304	0.328	0.396	0.044	0.271	0.058	0.914	0.046	0.259	0.001	0.039*	0.033	0.035*	0.001	0.010*	0.181	0.207
cg04981696	ABCC1	0.260	0.318	0.420	0.784	0.046	0.090	0.055	0.778	0.470	0.645	0.002	0.033*	0.657	0.736	0.000	0.004*	0.777	0.547
cg05102190	ZYX	0.116	0.122	0.972	0.880	0.039	0.084	0.056	0.360	0.301	0.926	0.025	0.077	0.338	0.365	0.005	0.030*	0.812	0.717
cg05131957	CRLS1	0.091	0.199	0.489	0.876	0.032	0.274	0.068	0.312	0.585	0.892	0.006	0.047*	0.995	0.780	0.018	0.069	0.483	0.196
cg05209527	SLC5A6	0.143	0.519	0.254	0.407	0.141	0.919	0.040	0.109	0.563	0.908	0.005	0.506	0.923	0.353	0.000	0.006*	0.478	0.317
cg06706068	RPUSD1	0.034	0.020*	0.477	0.970	0.533	0.052	0.032	0.268	0.090	0.748	0.023	0.049*	0.233	0.243	0.003	0.043*	0.851	0.586
cg07067744	BRSK2	0.782	0.974	0.454	0.760	0.093	0.104	0.038	0.963	0.389	0.782	0.003	0.030*	0.360	0.435	0.012	0.108	0.694	0.757
cg07112456	LRWD1	0.167	0.261	0.370	0.531	0.230	0.199	0.071	0.660	0.470	0.664	0.033	0.178	0.082	0.097	0.031	0.208	0.475	0.480
cg07953400	PIGQ	0.001	0.004*	0.625	0.452	0.233	0.005*	0.000	0.823	0.916	0.770	0.000	0.001*	0.250	0.343	0.013	0.041*	0.939	0.439
cg07956264	GPATCH3	0.702	0.693	0.026	0.068	0.000	0.028*	0.029	0.002*	0.112	0.493	0.009	0.023*	0.158	0.164	0.000	0.002*	0.282	0.232
cg08013262	INSR	0.582	0.678	0.482	0.695	0.031	0.046*	0.023	0.242	0.850	0.569	0.013	0.061	0.847	0.952	0.001	0.005*	0.859	0.992
cg09367046	ANGEL1	0.275	0.356	0.557	0.793	0.109	0.351	0.190	0.811	0.203	0.624	0.022	0.118	0.175	0.205	0.000	0.002*	0.198	0.188
cg10077144		0.722	0.544	0.467	0.283	0.006	0.203	0.029	0.084	0.645	0.736	0.007	0.138	0.950	0.711	0.002	0.004*	0.776	0.621
cg10178228	FRMD4B	0.566	0.705	0.482	0.603	0.447	0.937	0.668	0.196	0.005	0.055	0.078	0.357	0.240	0.270	0.000	0.005*	0.838	0.776
cg12289509	TUBE1	0.402	0.503	0.479	0.670	0.236	0.029*	0.019	0.921	0.676	0.683	0.001	0.002*	0.443	0.489	0.000	0.001*	0.624	0.833
cg12473838	SSBP1	0.004	0.167	0.500	0.711	0.419	0.928	0.000	0.192	0.000	0.664	0.001	0.030*	0.122	0.140	0.755	0.199	0.453	0.765
cg13291296	GPR125	0.652	0.802	0.697	0.967	0.034	0.101	0.064	0.256	0.063	0.211	0.010	0.028*	0.242	0.253	0.012	0.057	0.752	0.820
cg13397649	AFG3L2	0.090	0.227	0.678	0.749	0.003	0.809	0.305	0.079	0.133	0.385	0.038	0.295	0.898	0.948	0.017	0.082	0.301	0.156
cg13463639	SIGIRR	0.082	0.551	0.618	0.985	0.376	0.709	0.002	0.348	0.028	0.363	0.009	0.020*	0.375	0.275	0.980	0.730	0.298	0.431
cg13920768	PRDM12	0.278	0.431	0.539	0.635	0.004	0.101	0.035	0.065	0.855	0.221	0.016	0.095	0.278	0.347	0.007	0.040*	0.779	0.710
cg14214745	CRELD1	0.764	0.627	0.141	0.246	0.001	0.419	0.207	0.024*	0.022	0.196	0.048	0.218	0.883	0.713	0.041	0.267	0.314	0.359
cg14247318		0.405	0.309	0.206	0.361	0.052	0.009*	0.017	0.146	0.456	0.718	0.004	0.004*	0.224	0.215	0.011	0.031*	0.648	0.821
cg14451560	ARRDC1	0.132	0.129	0.282	0.480	0.075	0.191	0.117	0.452	0.044	0.182	0.022	0.076	0.040	0.047*	0.014	0.078	0.796	0.810
cg15226170	PMM1	0.894	0.780	0.422	0.625	0.024	0.354	0.136	0.352	0.511	0.911	0.012	0.095	0.302	0.203	0.001	0.009*	0.535	0.537

Illumina ID	Gene symbol	GLU		HOMAIN		TG		TC		HDL		LDL		GGT		ALT		AST	
		1#	2#	1#	2#	1#	2#	1#	2#	1#	2#	1#	2#	1#	2#	1#	2#	1#	2#
cg15317837	GTPBP4	0.920	0.942	0.194	0.550	0.005	0.682	0.507	0.282	0.012	0.244	0.166	0.460	0.650	0.708	0.016	0.254	0.127	0.472
cg15536552	ACSL4	0.001	0.439	0.001	0.045*	0.001	0.189	0.050	0.478	0.670	0.667	0.001	0.085	0.119	0.664	0.001	0.043*	0.071	0.431
cg15653194	LFNG	0.167	0.052	0.190	0.843	0.000	0.001*	0.006	0.010*	0.124	0.320	0.001	0.001*	0.840	0.955	0.016	0.453	0.001	0.111
cg16105594	MEF2C	0.228	0.481	0.701	0.832	0.042	0.234	0.067	0.437	0.020	0.064	0.002	0.022*	0.411	0.500	0.026	0.124	0.086	0.213
cg16261091	HEXDC	0.722	0.620	0.073	0.146	0.005	0.315	0.242	0.110	0.093	0.465	0.044	0.118	0.097	0.095	0.004	0.036*	0.561	0.614
cg16357287	SEH1L	0.574	0.745	0.092	0.138	0.081	0.183	0.110	0.446	0.126	0.361	0.008	0.025*	0.773	0.709	0.000	0.003*	0.644	0.386
cg16398128	ZNF622	0.410	0.717	0.339	0.352	0.003	0.022*	0.005	0.058	0.365	0.766	0.000	0.001*	0.976	0.859	0.000	0.001*	0.809	0.764
cg16416718	CAMTA1	0.001	0.004*	0.739	0.772	0.200	0.010*	0.001	0.778	0.387	0.558	0.000	0.001*	0.053	0.069	0.031	0.079	0.984	0.313
cg16487280	MYBL2	0.082	0.070	0.708	0.744	0.183	0.112	0.064	0.488	0.989	0.067	0.006	0.027*	0.671	0.497	0.081	0.624	0.004	0.060
cg17162475	C6orf150	0.317	0.328	0.201	0.465	0.052	0.507	0.341	0.874	0.052	0.618	0.032	0.165	0.562	0.635	0.000	0.008*	0.611	0.313
cg17176517	SNX4	0.349	0.639	0.406	0.446	0.255	0.182	0.042	0.821	0.291	0.593	0.005	0.062	0.563	0.713	0.006	0.030*	0.715	0.484
cg18570553	PRR15	0.042	0.098	0.444	0.310	0.028	0.043*	0.008	0.387	0.640	0.712	0.001	0.009*	0.063	0.084	0.005	0.035*	0.527	0.705
cg18848688	LIFR	0.885	0.925	0.125	0.242	0.003	0.064	0.051	0.102	0.023	0.175	0.005	0.012*	0.224	0.221	0.002	0.022*	0.651	0.826
cg19189310	RPS10	0.398	0.564	0.453	0.711	0.062	0.150	0.052	0.953	0.205	0.964	0.009	0.086	0.200	0.239	0.005	0.075	0.292	0.224
cg19634213	PTEN	0.194	0.497	0.494	0.932	0.900	0.353	0.102	0.213	0.483	0.651	0.010	0.092	0.297	0.356	0.001	0.002*	0.236	0.447
cg19878987	LDHB	0.321	0.532	0.328	0.574	0.086	0.136	0.034	0.691	0.477	0.932	0.008	0.087	0.176	0.240	0.001	0.003*	0.197	0.218
cg21786114	EHMT2	0.344	0.374	0.953	0.367	0.023	0.073	0.060	0.841	0.363	0.484	0.004	0.029*	0.600	0.654	0.001	0.018*	0.809	0.483
cg22185268	COMMD4	0.943	0.744	0.548	0.618	0.007	0.180	0.058	0.108	0.299	0.842	0.001	0.019*	0.329	0.431	0.001	0.008*	0.467	0.844
cg22746421		0.798	0.779	0.030	0.105	0.130	0.237	0.205	0.633	0.011	0.241	0.021	0.054	0.302	0.289	0.002	0.038*	0.163	0.527
cg23224405	DUSP16	0.873	0.594	0.099	0.062	0.024	0.256	0.053	0.351	0.099	0.194	0.002	0.054	0.147	0.199	0.000	0.001*	0.197	0.435
cg24199050	GTSE1	0.064	0.175	0.949	0.862	0.012	0.006*	0.001	0.129	0.719	0.984	0.000	0.001*	0.754	0.988	0.004	0.013*	0.717	0.190
cg24689754	C19orf62	0.357	0.466	0.273	0.341	0.147	0.607	0.366	0.576	0.102	0.183	0.007	0.045*	0.731	0.593	0.001	0.005*	0.368	0.104
cg25295726	FUT11	0.685	0.906	0.175	0.314	0.056	0.231	0.094	0.748	0.030	0.184	0.007	0.050	0.112	0.130	0.003	0.040*	0.699	0.746
cg25456633		0.613	0.938	0.003	0.003*	0.080	0.581	0.235	0.649	0.296	0.688	0.085	0.377	0.626	0.742	0.001	0.012*	0.893	0.758
cg25818813	MERTK	0.131	0.253	0.968	0.926	0.087	0.037*	0.015	0.264	0.848	0.545	0.000	0.002*	0.478	0.550	0.000	0.001*	0.179	0.513
cg26105057	PAN2	0.843	0.972	0.305	0.831	0.029	0.122	0.161	0.401	0.107	0.656	0.058	0.082	0.155	0.137	0.000	0.002*	0.522	0.167
cg26309655	TARS2	0.103	0.299	0.820	0.667	0.065	0.172	0.032	0.301	0.671	0.670	0.006	0.077	0.391	0.514	0.004	0.008*	0.757	0.542
g22721468	SH3BP5L	0.097	0.225	0.616	0.649	0.232	0.106	0.028	0.816	0.618	0.787	0.000	0.009*	0.465	0.569	0.001	0.008*	0.643	0.882

1# – Uni-variate p; 2# – Multi-variate; p* p<0.05, adjusted by sex, age and BMI.

References:

1. Chalasani N, Younossi Z, Lavine JE et al: The diagnosis and management of nonalcoholic fatty liver disease: Practice guidance from the American Association for the Study of Liver Diseases. *Hepatology*, 2018; 67(1): 328–57
2. Younossi ZM, Koenig AB, Abdelatif D et al: Global epidemiology of nonalcoholic fatty liver disease. Meta-analytic assessment of prevalence, incidence, and outcomes. *Hepatology*, 2016; 64(1): 73–84
3. Fan JG, Kim SU, Wong VW: New trends on obesity and NAFLD in Asia. *J Hepatol*, 2017; 67(4): 862–73
4. McPherson S, Hardy T, Henderson E et al: Evidence of NAFLD progression from steatosis to fibrosing-steatohepatitis using paired biopsies: Implications for prognosis and clinical management. *J Hepatol*, 2015; 62(5): 1148–55
5. Tian JB, Zhong R, Liu C et al: Association between bilirubin and risk of nonalcoholic fatty liver disease based on a prospective cohort study. *Sci Rep*, 2016; 6: 310006
6. Zimmer V, Lammert F: Genetics and epigenetics in the fibrogenic evolution of chronic liver diseases. *Best Pract Res Clin Gastroenterol*, 2011; 25(2): 269–80
7. Podrini C, Borghesan M, Greco A et al: Redox homeostasis and epigenetics in non-alcoholic fatty liver disease (NAFLD). *Curr Pharm Design*, 2013; 19(15): 2737–46
8. Illingworth RS, Bird AP: CpG islands – ‘A rough guide’. *Febs Lett*, 2009; 583(11): 1713–20
9. Neuschwander-Tetri BA, Loomba R, Sanyal AJ et al: Farnesoid X nuclear receptor ligand obeticholic acid for non-cirrhotic, non-alcoholic steatohepatitis (FLINT): A multicentre, randomised, placebo-controlled trial. *Lancet*, 2015; 385(9972): 956–65
10. Cordero P, Campion J, Milagro FI, Martinez JA: Transcriptomic and epigenetic changes in early liver steatosis associated to obesity: Effect of dietary methyl donor supplementation. *Mol Genet Metab*, 2013; 110(3): 388–95
11. Zeybel M, Hardy T, Robinson SM et al: Differential DNA methylation of genes involved in fibrosis progression in non-alcoholic fatty liver disease and alcoholic liver disease. *Clin Epigenetics*, 2015; 7: 25
12. Ahrens M, Ammerpohl O, von Schonfels W et al: DNA methylation analysis in nonalcoholic fatty liver disease suggests distinct disease-specific and remodeling signatures after bariatric surgery. *Cell Metab*, 2013; 18(2): 296–302
13. Murphy SK, Yang HN, Moylan CA et al: Relationship between methylome and transcriptome in patients with nonalcoholic fatty liver disease. *Gastroenterology*, 2013; 145(5): 1076–87
14. Gallego-Duran R, Romero-Gomez M: Epigenetic mechanisms in non-alcoholic fatty liver disease: An emerging field. *World J Hepatol*, 2015; 7(24): 2497–502
15. Hardy T, Zeybel M, Day CP et al: Plasma DNA methylation: A potential biomarker for stratification of liver fibrosis in non-alcoholic fatty liver disease. *Gut*, 2017; 66(7): 1321–28
16. Nano J, Ghanbari M, Wang W et al: Epigenome-wide association study identifies methylation sites associated with liver enzymes and hepatic steatosis. *Gastroenterology*, 2017; 153(4): 1096–106e2
17. Bedossa P, Poitou C, Veyrie N et al: Histopathological algorithm and scoring system for evaluation of liver lesions in morbidly obese patients. *Hepatology*, 2012; 56(5): 1751–59
18. Du P, Kibbe WA, Lin SM: Lumi: A pipeline for processing Illumina microarray. *Bioinformatics*, 2008; 24(13): 1547–48
19. Dupuy D, Bertin N, Hidalgo CA et al: Genome-scale analysis of *in vivo* spatiotemporal promoter activity in *Caenorhabditis elegans*. *Nat Biotechnol*, 2007; 25(6): 663–68
20. Draghici S, Khatri P, Tarca AL et al: A systems biology approach for pathway level analysis. *Genome Res*, 2007; 17(10): 1537–45
21. Wilhelm-Benartzi CS, Koestler DC, Karagas MR et al: Review of processing and analysis methods for DNA methylation array data. *Br J Cancer*, 2013; 109(6): 1394–402
22. Dunham I, Kundaje A, Aldred SF et al: An integrated encyclopedia of DNA elements in the human genome. *Nature*, 2012; 489(7414): 57–74
23. Kusminski CM, Holland WL, Sun K et al: MitoNEET-driven alterations in adipocyte mitochondrial activity reveal a crucial adaptive process that preserves insulin sensitivity in obesity. *Nat Med*, 2012; 18(10): 1539–49
24. Mikeska T, Craig JM: DNA methylation biomarkers: Cancer and beyond. *Genes*, 2014; 5(3): 821–64
25. Pratt DS, Kaplan MM: Primary care: Evaluation of abnormal liver-enzyme results in asymptomatic patients. *N Engl J Med*, 2000; 342(17): 1266–71
26. van Beek JHDA, Lubke GH, de Moor MHM et al: Heritability of liver enzyme levels estimated from genome-wide SNP data. *Eur J Hum Genet*, 2015; 23(9): 1223–28
27. Liu WS, Baker RD, Bhatia T et al: Pathogenesis of nonalcoholic steatohepatitis. *Cell Mol Life Sci*, 2016; 73(10): 1969–87
28. Alkhoury N, Eng K, Lopez R, Nobili V: Non-high-density lipoprotein cholesterol (non-HDL-C) levels in children with nonalcoholic fatty liver disease (NAFLD). *Springerplus*, 2014; 3: 407
29. Koppe SWP: Obesity and the liver: Nonalcoholic fatty liver disease. *Transl Res*, 2014; 164(4): 312–22
30. Stroka KM, Levitan I, Aranda-Espinoza H: OxLDL and substrate stiffness promote neutrophil transmigration by enhanced endothelial cell contractility and ICAM-1. *J Biomech*, 2012; 45(10): 1828–34
31. Kwok R, Tse YK, Wong GL et al: Systematic review with meta-analysis: Non-invasive assessment of non-alcoholic fatty liver disease – the role of transient elastography and plasma cyokeratin-18 fragments. *Aliment Pharmacol Ther*, 2014; 39(3): 254–69
32. Krishnan J, Danzer C, Simka T et al: Dietary obesity-associated Hif1a activation in adipocytes restricts fatty acid oxidation and energy expenditure via suppression of the Sirt2-NAD+ system. *Genes Dev*, 2012; 26(3): 259–70
33. Song CY, Zeng X, Wang Y et al: Sophocarpine attenuates toll-like receptor 4 in steatotic hepatocytes to suppress pro-inflammatory cytokines synthesis. *J Gastroen Hepatol*, 2015; 30(2): 405–12
34. Cui M, Xiao ZL, Sun BD et al: Involvement of cholesterol in hepatitis B virus X protein-induced abnormal lipid metabolism of hepatoma cells via up-regulating miR-205-targeted ACSL4. *Biochem Bioph Res Commun*, 2014; 445(3): 651–55
35. Zhang RN, Pan Q, Zheng RD et al: Genome-wide analysis of DNA methylation in human peripheral leukocytes identifies potential biomarkers of non-alcoholic fatty liver disease. *Int J Mol Med*, 2018; 42(1): 443–52
36. European Association for the Study of the Liver (EASL); European Association for the Study of Diabetes (EASD); European Association for the Study of Obesity (EASO). EASL-EASD-EASO Clinical Practice Guidelines for the management of nonalcoholic fatty liver disease. *J Hepatol*, 2016; 64(6): 1388–402
37. Bedossa P: Utility and appropriateness of the fatty liver inhibition of progression (FLIP) algorithm and steatosis, activity, and fibrosis (SAF) score in the evaluation of biopsies of nonalcoholic fatty liver disease. *Hepatology*, 2014; 60: 565–75
38. Das M, Sha J, Hidalgo B et al: Association of DNA methylation at CPT1A locus with metabolic syndrome in the genetics of lipid lowering drugs and diet network (GOLDN) study. *PLoS One*, 2016; 11(1): e0145789
39. Paradies G, Paradies V, Ruggiero FM, Petrosillo G: Oxidative stress, cardiometabolic and mitochondrial dysfunction in nonalcoholic fatty liver disease. *World J Gastroenterol*, 2014; 20(39): 14205–18
40. Dolinsky VW, Cole LK, Sparagna GC, Hatch GM: Cardiac mitochondrial energy metabolism in heart failure: Role of cardiometabolic and sirtuins. *Biochim Biophys Acta*, 2016; 1861(10): 1544–54